OPTIMIZED *FTR* PORTFOLIO CONSTRUCTION: THE SPECULATOR'S PROBLEM

BY

DIMITRA APOSTOLOPOULOU

THESIS

Submitted in partial fulfillment of the requirements
for the degree of Master of Science in Electrical and Computer Engineering
in the Graduate College of the
University of Illinois at Urbana-Champaign, 2011

Urbana, Illinois

Adviser:

Professor George Gross

ABSTRACT

In this thesis, we propose a systematic methodology to construct an optimized financial transmission rights (FTR) portfolio for the speculator, who purchases FTR holdings in order to have returns that are as good as possible. The conventional approach of selecting the FTR in a portfolio requires the exhaustive evaluation of all the possible FTR combinations, which in a large-scale network is computationally too demanding a task, particularly when the wide variations in the behavior of the locational marginal price (LMP) differences of nodes over the many hours of the holding period are taken into account. In order to make the speculator's problem more manageable, we recast the problem into a form that allows us to exploit the salient characteristics of power systems, the topological nature of the underlying network and the historical data, so as to gain mathematical insights that we apply to develop the proposed scheme. The speculator returns are collected from the hourly day ahead markets (DAMs) only for those hours that the grid is congested, i.e., the flows on one or more lines are at their maximum limits. Each MW flowing through those lines incurs a transmission usage cost. Unlike a physical transaction from a source node to a sink node that holds FTR in the amount of the flow and receives reimbursement for the transmission usage charges from the independent grid operator (IGO), the speculator who holds FTR for the same node pair simply receives those revenues, because of lack of physical flows. Thus, the identification of congested lines is a key step in the construction methodology. So, rather than focusing on the LMP differences of node pairs to choose FTR, we select node pairs such that the selected congested lines are on their paths from the source nodes to the sink nodes. Conceptually, we specify FTR such that transactions with same node pairs and amounts induce real power flows on the selected congested lines. The strategy of the speculator is to select each congested line and his level of participation on the congested flows on the line. In practice, the speculator

cannot do this for all the congested lines, because that would imply the acquisition of too large a number of *FTR*, whose premiums add to his costs and, thus, lower his returns. Under the assumption that the past behavior continues in the future, he judiciously chooses a subset of lines whose transmission usage costs exceeded the speculator's specified price and time fraction thresholds historically. This subset forms the basis of the optimized *FTR* portfolio construction. In our proposed scheme, we construct the *FTR* portfolio with minimum number of node pairs; i.e., we find the minimum number of transactions that induce the desired real power flows on the subset of selected lines. To demonstrate the computational efficiency of the construction algorithm, we select a subset of nodes to specify the *FTR* node pairs in the portfolio. The manageability of the problem is further aided by focusing on a small number of node pairs. Fewer node pairs improve the manageability. The recasting of the problem in terms of congested lines, rather than *LMP* differences of node pairs, results in a simplified solution methodology that is amenable to practical implementation. We have extensively tested the proposed methodology on multiple test systems and we discuss representative case study results. The results on three test systems, including the *PJM ISO* network, illustrate the effectiveness of the proposed approach and provide insights into the nature of the problem.

To my parents

ACKNOWLEDGMENTS

I thank my adviser, Professor George Gross, for the guidance and support he provided during this entire period. I appreciate his help in better articulating my thoughts and our numerous discussions. I also thank Teoman Güler for providing a very fruitful internship experience. He introduced me to the complexity of *FTR* issues and assigned me challenging problems to make some dent in the solution. I thank all the students in the power group for their encouragement and advice. Finally, I thank my family for supporting me in all possible ways during my studies.

TABLE OF CONTENTS

LIST OF TABLES

LIST OF FIGURES

LIST OF ABBREVIATIONS

CRR	Congestion Revenue Rights
CAISO	California *ISO*
DAM	Day Ahead Market
ERCOT	Electricity Reliability Council of Texas
FTR	Financial Transmission Rights
IGO	Independent Grid Operator
ISF	Injection Shift Factor
ISO	Independent Service Operator
ISONE	*ISO* New England
LMP	Locational Marginal Price
LODF	Line Outage Distribution Factor
NYISO	New York *ISO*
OPF	Optimal Power Flow
OTDF	Outage Transfer Distribution Factor
PTDF	Power Transfer Distribution Factor
RTO	Regional Transmission Operator
TSO	Transmission Service Operator
TCC	Transmission Congestion Contract
TUCDC	Transmission Usage Cost Duration Curve

CHAPTER 1

INTRODUCTION

In this chapter, we set the stage for the work presented in this thesis. Our research interests lie in the construction of *FTR* portfolios for speculation purposes. We start by discussing the motivation for, and the background behind, our research so as to allow the reader to better understand the nature of the problem considered and the solution we have developed. We also provide a brief description of the current state-of-the-art in the field of *FTR*. We then summarize the scope and the contribution of this work and outline the contents of the rest of the thesis.

1.1 Overview of Financial Transmission Rights (*FTR*)

The new electric power paradigm provides a competitive market environment for the trading of electricity between buyers and sellers and ultimately manages the physical delivery of bulk electricity. Independent grid operators (*IGO*s) such as regional transmission organizations (*RTO*s), independent system operators (*ISO*s) and transmission system operators (*TSO*s) are responsible for ensuring reliable operations, maintenance, and expansion of a geographically widespread grid and for implementing appropriate mechanisms for transmission pricing that lead to the efficient and nondiscriminatory use of the transmission grid by all market participants. Transmission service is the most critical element in making competitive electricity markets work effectively. However, when the transactions that parties wish to schedule result in the violation of a transmission constraint, the system becomes congested and the *IGO* must take action to relieve constraint violations. Such transmission constraints include thermal limits, voltage constraints, stability restrictions on flows and emergency limits for specified contingency cases. The actions that the *IGO* takes to relieve congestion are elements of congestion management, and include redispatch of the units and load curtailment. The locational pricing model that makes use of nodal prices in electricity markets is widely used by many *IGO*s for short-term congestion management. Such prices are the outcomes of the day-ahead markets (*DAM*s) that the *IGO* clears based on the sell offers, the buy bids and the bilateral transactions' willingness to pay for transmission service. The market clearing explicitly considers transmission network constraints, and so the market outcomes in terms of the locational marginal prices (*LMP*s) reflect the impacts of congestion in the grid. Indeed, the *LMP* may be different at each grid node [1]. *LMP*s may differ at each location in the presence of transmission congestion, since transmission congestion restricts energy flows from low-cost generation from meeting the loads. Congestion costs, collected by the *IGO* from the market participants as congestion rents, are evaluated in terms of the *LMP* differences and may have serious impacts on costs of electricity. For example, we show in Fig. 1.1 the costs in three North American *ISO*s for the years 2000-2006. We note that these costs have reached as high as two billion dollars for the *PJM ISO* in 2005. The *LMP* at each node determines

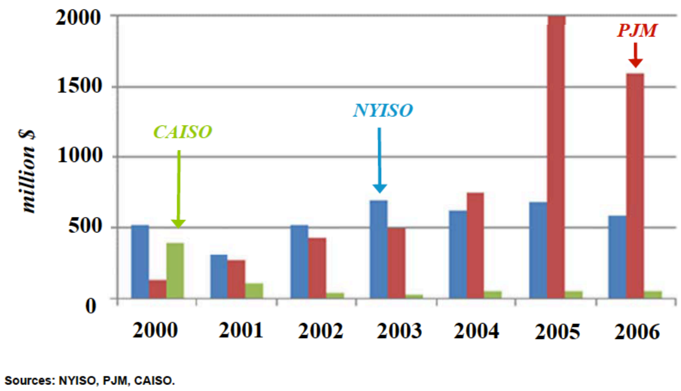

Figure 1.1: Congestion costs in *PJM ISO*, *CAISO* and *NYISO* from 2000-2006

the marginal cost of supplying an additional *MW* of load at that node for an hour, and so each market participant buys or sells energy at the *LMP* at a node for that hour. However, there is great volatility associated with the *LMP*s as is evident from Fig. 1.2 [2]. Such volatility in *LMP*s results in uncertainty in *LMP* differences and, in turn, in uncertainty in congestion rents. This uncertainty creates the need for hedging instruments. One such

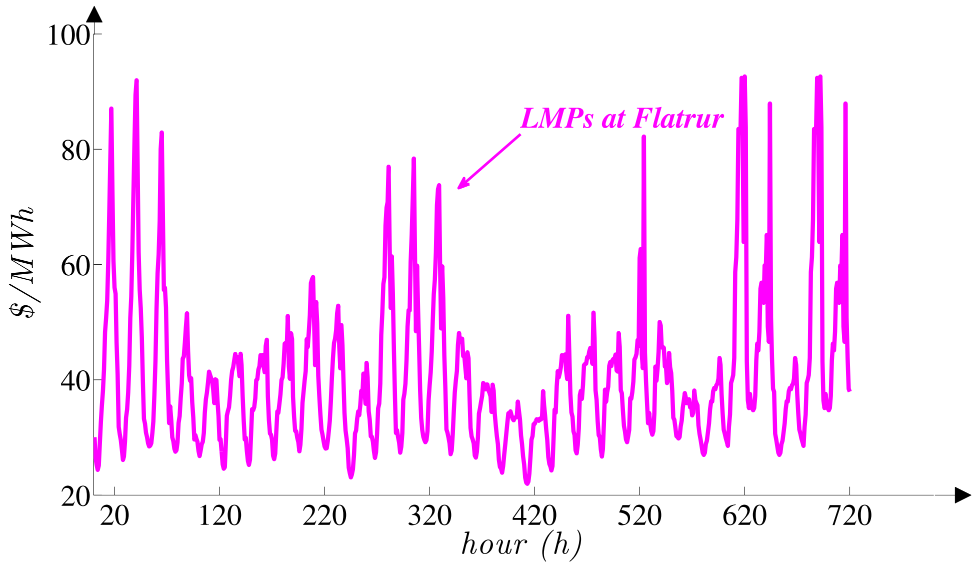

Figure 1.2: The plot of the hourly *LMP*s at the Flatrur bus in the *PJM ISO* network during September 2010

instrument is financial transmission rights or *FTR*, also known as transmission congestion contract (*TCC*) in the *NYISO* and congestion revenue rights (*CRR*) in the California *ISO* (*CAISO*) and the Electricity Reliability Council of Texas (*ERCOT*). *FTR* are successfully implemented in many *IGO*s, including the *PJM*, New York, New England and Midwest *ISO*s. *FTR* entitle their holders to receive reimbursement from the *IGO* for the value of congestion as established by the *LMP* difference in the *DAM*. Thus, the holder of *FTR* for a specified *to* and *from* node pair with a physical transaction with the identical injection and withdrawal node pair is not impacted financially by the *LMP* difference of the *to* and *from* node prices as long as the *FTR* for that node pair is in the same *MW* amount as his physical delivery. The *IGO* reimburses the *FTR* holder the same amount it collects in congestion rents for that transaction.

FTR may be understood as financial instruments specified by their source nodes, sink nodes and the *MW* amounts. *FTR* are strictly directional in nature and that information is given by the source and sink node pair specification. *FTR* are further characterized by the holding period, which is defined by the start and the end times and the class. The class refers to the coverage subperiods and, typically, comes in three categories: on-peak, off-peak and around the clock. The *FTR* tool is further categorized as either a contract or an option type. The *FTR* contracts provide reimbursements to the holder whenever the congestion is in the direction specified by the *FTR*. However, the contracts turn into a liability whenever the *LMP* difference of the source and the sink nodes is negative, i.e., the congestion is in the opposite direction. The *FTR* options are only exercised when the reimbursements are beneficial to the holder.

The acquisition of *FTR* is either through grandfathering to "stakeholders" by the *IGO* or through sales conducted by the *IGO* or secondary markets. The *IGO* runs periodic auctions where it sells *FTR* holdings to buyers who bid for the offered quantities. The buyers may either be hedgers or speculators. Hedgers buy *FTR* for insurance to receive reimbursements for any congestion rents incurred as a result of congestion in the grid with their transactions. Speculators purchase *FTR* even in the absence of physical flows in order to maximize their earnings. Speculator participation in *FTR* auctions results in a more competitive environment and may lead to higher *FTR* premiums. The market participants, hedgers and speculators, submit their bids for *FTR* by specifying the sink and source node pairs, the desired *MW* amounts and the maximum willingness to pay in $\$/MW$-duration for each node pair. However, the market participants may only choose node pairs from a specified *from* and *to* nodes, the so-called pricing node set. The objective of the *IGO* is to maximize the bid-based values of awarded *FTR* that are simultaneously feasible without violating any system and operational constraints for the *FTR* duration. The outcomes of the *FTR* auctions determine the actual *MW* amounts and premium prices of awarded *FTR*. The *IGO* is responsible for revenue adequacy, i.e., to ensure that the collected *FTR* premiums are sufficient to pay off all future reimbursements for the associated holding period.

In *PJM ISO*, *FTR* auctions offer multiple products in terms of duration: one month, three months, one year and three year holding periods; various classes and contract and/or option type. Moreover, the primary *FTR* auctions in which new *FTR* are issued fall in three categories—long-term, annual and monthly—that provide various *FTR* products. As an example, we provide a listing in Table 1.1 of the various primary *FTR* auctions and the associated products in the *PJM ISO*. Each auction offers *FTR* of the three classes. In the monthly auctions, four possible squarters are offered: June 1 to August 31, September 1 to November 30 and March 1 to May 31.

Table 1.1: *FTR* product types in the *PJM FTR* auction of year y for long-term and annual auctions and month m for the monthly auction

auction type	*long-term*	*annual*	*monthly*
date	June, October	April	every month
***FTR* capability auctioned**	system capability	system *FTR* capability minus cleared long-term	residual capability of the system
annual number of auctions	1 auction with 2 rounds	one auction with 4 rounds	12 monthly auctions
***FTR* product type**	contract	contract, option	contract, option
***FTR* holding period**	*three year*:	*one year*	*one month*
	$06/01/y+1$ to $05/31/y+4$	$06/01/y$ $05/31/y+1$	$m/01/y$ $m/30\text{-}31/y$
	one year:		$m+1/01/y$ $m+1/30\text{-}31/y$
	$06/01/y+1$ to $05/31/y+2$		$m+2/01/y$ $m+2/30\text{-}31/y$
	$06/01/y+2$ to $05/31/y+3$		*three months*:
	$06/01/y+3$ to $05/31/y+4$		any complete quarter remaining in y

Besides the primary markets, there are secondary markets where *FTR* holders may resell their *FTR* in part or in full. In these markets, *FTR* may be split into products with shorter holding periods or *MW* amounts as long as their sum does not violate the amount of the original *FTR* holdings.

The *FTR* auction determines for each specified product in terms of type, node pair, class and holding period, the *MW* quantities allocated to the buyers and the premium price in $\$/MW$-duration. The associated revenues for the *FTR* holders are determined by the outcomes of the *DAM*s that are held during the holding period. We briefly review the *DAM*'s structure and outcomes to provide the setting in which the impacts of holding *FTR* are evaluated.

We consider the centralized pool market structure for the *DAM*, which is widely adopted in North America. The *IGO* collects the sealed offers submitted by the sellers specifying the quantities and willingness to sell, the sealed bids by the buyers indicating the quantities desired and the willingness to buy, and the amount of transmission service requested by bilateral transactions and their willingness to buy. The *IGO* uses this information to clear the market and determines the outcomes to meet the demand by maximizing social welfare. The outcomes specify for each buyer (seller) the amount bought (sold) and the price and the amount of transmission service to the transactions requesting the service. The physical transmission constraints, along with the operational and security considerations for the operation of the power system, are explicitly taken into account in determining the outcomes. As such, the *LMP*s reflect the impacts of the transmission constraints and are used to determine the congestion rents collected and the reimbursements to the *FTR* holders.

1.2 Review of the State of the Art in *FTR*

The basic concept of *FTR* was first introduced by Hogan in a paper that set out the mathematical framework for the analysis of the *FTR* tool [3]. A more detailed treatment of *FTR* issues was developed later in 2002 [4]. The implementation of *FTR* in various *IGO*s was accompanied by rules particular to each jurisdiction [5], [6], [7], [8]. These implementations provide a good range of realizations of the basic concepts of *FTR*. A comparative analysis of the *FTR* implementations around the world would provide additional insights on different methodologies and rules that have been discussed in [9].

While the original objective in the introduction of *FTR* was to provide insurance to entities with physical transactions, and in this way, to provide hedging for those transactions, the use of *FTR* for speculation has been discussed in [10]. The *IGO*s are keen to promote the liquidity of the *FTR* markets and include the participation of entities without physical flows, so as to make the *FTR* auctions more competitive. The original introduction for *FTR* was for *FTR* contracts, which become a liability whenever the *LMP* differences between the sink and source node pair become negative. Such outcomes led to the investigation of the applicability of options to *FTR* [11]. No major hurdles with the introduction of *FTR* options in the *ISONE* market were identified in the *ISO* New England (*ISONE*) jurisdiction and the specific advantages and risk aspects are detailed in [11].

A bidding strategy in *FTR* auctions, under the assumption of the characteristics of the *LMP* differences by analytical probability distributions, was developed in [12]. The salient mathematical aspects of *FTR* auction clearing mechanisms and analysis of the *FTR* auction outcomes were topics of various papers [13], [14], [15], [16]. A very useful and comprehensive survey paper assessing the *FTR* literature is [17].

Since their introduction, *FTR* became a well-established financial tool in electricity markets. Their deployment is important to creating smoothly operating electricity markets. The increasing utilization of *FTR* led to their consideration in the analysis of transmission expansion planning and investment decisions. Several papers focus on the need to address *FTR* issues associated with the expansion of the transmission network. Hogan identified the importance of *FTR* signal for transmission expansion [18]. The use of long-term *FTR* to create incentives for transmission investments was discussed in [19], [20]. The efficient implementation of such a scheme in small incremental investments without major impact on the market value of *FTR* was described in [21]. Such a scheme underlines the ability of *FTR* to provide useful economic signals for transmission investment.

Thus far, the issue of constructing a portfolio of *FTR* for speculative purposes has not been studied and reported in the literature. Since the role of speculators is important in the competitiveness of *FTR* auction markets and their participation adds to the liquidity of such markets, such issues are certainly of interest in the *FTR* realm. We address in this thesis the analysis and the solution approach of the speculator problem. In the next section we describe the problem and summarize our proposed approach to the construction of the optimized *FTR* portfolio for the speculator.

1.3 Nature of the Problem and Contributions of the Thesis

A speculator purchases *FTR* holdings in *FTR* auctions in order to have returns that are as good as possible. The outcomes of the *FTR* auction, which determine the *FTR* premiums, do not solely depend on speculator, since they are influenced by the behavior of the other market participants, speculators and hedgers, as well as the supply of *FTR* offered. Moreover, as the speculator may not participate in the *DAM*s during the holding periods, he has no control over the revenues emanating from the *FTR* holdings. There is uncertainty associated with the *FTR* revenues since the outcomes of the *DAM*s are uncertain. The speculator purchases *FTR* at a point in time for use during the holding period and faces uncertainty in both the premium prices and the revenues of the future holding period. We depict in Fig. 1.3 the timeline of the *FTR* purchase and use. In light of the uncertainty and the

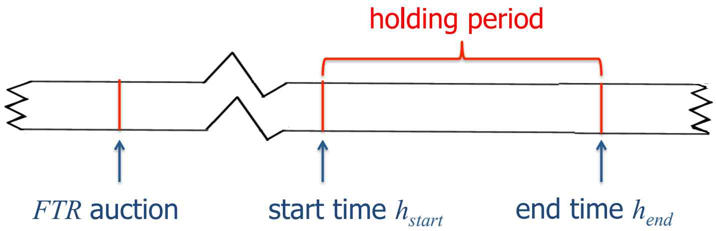

Figure 1.3: The holding period associated with the *FTR* acquisition

large number of possible combinations of *FTR* he may purchase, the speculator faces a challenging problem in constructing a "good" *FTR* portfolio. The speculator's problem is too unconstrained, since there is not enough information about the future stream of revenues. There is a need to find a way to reduce the state space of solutions. An exhaustive evaluation of all the possible combinations in a large-scale network is computationally too demanding a task, particularly when the consideration of the wide variations in the behavior of the *LMP* differences of nodes over the many hours of the holding period are taken into account.

Rather, we focus on solving the portfolio construction problem for a simplified form where we consider the acquisition in a single auction and the purchase of *FTR* contracts for a specified holding period. Also, we do not consider any other *FTR* holdings of the speculator.

We introduce some mathematical notation to allow us to make more concrete statements about the nature of the problem and the solution approach we propose. We denote the *FTR* with source (sink) node i (j) in the *MW* amount γ by the triplet

$$\Gamma = \{i, j, \gamma\} \ . \tag{1.1}$$

The speculator's problem concerns the identification of the elements of the optimized *FTR* portfolio $\mathscr{F}$, where

$$\mathscr{F} \triangleq \{\Gamma_1, \ldots, \Gamma_K\} \ . \tag{1.2}$$

For each $\Gamma_k \in \mathscr{F}$, we need to specify the triplet elements i_k, j_k and γ_k, where $k = 1, \ldots, K$. However, even for the simplified setting of a single holding period, the number of *FTR* combinations is huge. In order to make the speculator's problem more manageable, we recast it into a form that allows us to exploit the salient characteristics of power systems, the topological nature of the underlying network, the historical data, and their economic interpretation, so as to gain mathematical insights that we apply in the proposed methodology. A grid has certain lines that are congested; i.e., the flows on the lines are at the maximum limits. We associate with a line where the flow is at its limit the economic term that indicates the marginal benefit obtained from the last MW in the flow that results in the flow at its limiting value. The charge for using the congested line is set at its marginal benefit and the IGO assesses this charge from every transaction that flows on that line. This charge is called the per unit transmission usage cost for a congested line. From now on we will simply refer to it as transmission usage cost. Indeed, the congestion rents collected by the IGO are the sum of the transmission usage costs multiplied by the real power flow on all congested lines, which are incurred by all the transactions, whose flows in part or in whole, are along these lines. A transaction from source node i to sink node j that has FTR in the amount of the flows receives reimbursement for the transmission usage charges from the IGO. In this way, the uncertainty in the nodal price difference during the FTR holding period provides the assurance, once the FTR premium is paid, that there are no additional charges for transmission usage. Similarly, a speculator who holds FTR for the same node pair receives revenues equal to the additional charges for the amount in the FTR holding, even in the absence of physical flows. Such revenues are exactly what the speculator wishes to maximize, by also taking into consideration the associated FTR premiums. Thus, the identification of congested lines is a key step in the construction methodology. We therefore focus on a portfolio construction strategy that allows the speculator to include FTR node pairs with paths that have congested lines. From a study of historical data, a subset of lines that, from past behavior, get congested may be identified. Such lines result in FTR revenues whenever they belong to paths between the source and sink node pair of FTR holdings of the speculator.

A particularly effective way to select lines in the subset is to construct transmission usage cost duration curves ($TUCDC$s) obtained by sorting the hourly cost data from highest to lowest. The $TUCDC$ abstracts out time and, when transmission usage cost values in $\$/MWh$ are the ordinate and the hours the abscissa, is monotonically non-increasing. We interpret a point (h, ξ) on the $TUCDC$ as follows. If the historical data set has H hours, then for the fraction h/H of the time, the transmission usage cost exceeds

ξ $\$/MWh$. The area under the $TUCDC$ gives the total congestion charges on the line collected for each MW of flow over the H hours. We use the $TUCDC$ to identify lines that exceed two price and time fraction thresholds specified by the speculator. We identify lines with high past values of transmission congestion charges and call the associated transmission constraints as chronic. The $TUCDC$ are also useful to identify those lines that in the past had very high values of transmission usage cost for a small portion of the total hours. The transmission constraints of these lines are called outage driven constraints. We make this concept more concrete by illustrating with data we collected on the PJM ISO system for the year 2010. Our analysis indicates that only 294 out of 19,787 lines get congested for one or more hours of the year and that the highest fraction of time that any line is congested is 30% of the 8760 hours of the year. In Fig. 1.4a, we depict the duration curves of lines whose transmission usage cost exceeds the two thresholds, and in Fig. 1.4b the duration curves of lines that do not.

The use of historical data may provide additional insights into the nature of congestion in terms of the key causal factor. Such information is useful because whenever a similar situation would arise in the future, we would know which lines would get congested. We choose the historical data accordingly to be well fitted with the specific holding period. Based on past experience, we focus on three main causal factors: demand levels, fuel price trends and specific changes in topology. Chronic constraints are usually driven by demand levels and fuel price trends. When the demand reaches high levels, we try to meet it with the cheapest generation, which might lead to having congested lines near the cheapest generation. We should be careful since if the demand is met by local resources, the transmission system is not burdened and no congestion arises. According to the same notion, the fuel price trends determine which generation is cheaper. Some regulation of coal may make coal units more expensive than gas units. For example, if we have two areas, one with generation based on coal and the other on gas, the lines connecting the two areas might get congested if the price difference between the two resources is large making one generation a lot cheaper than the other. The outage driven constraints bind when a generation or a line outage occurs. A line outage affects the remaining lines differently, depending on the grid structure. A particularly useful measure is the impact of a line outage on other lines as measured by a sensitivity factor known as the line outage

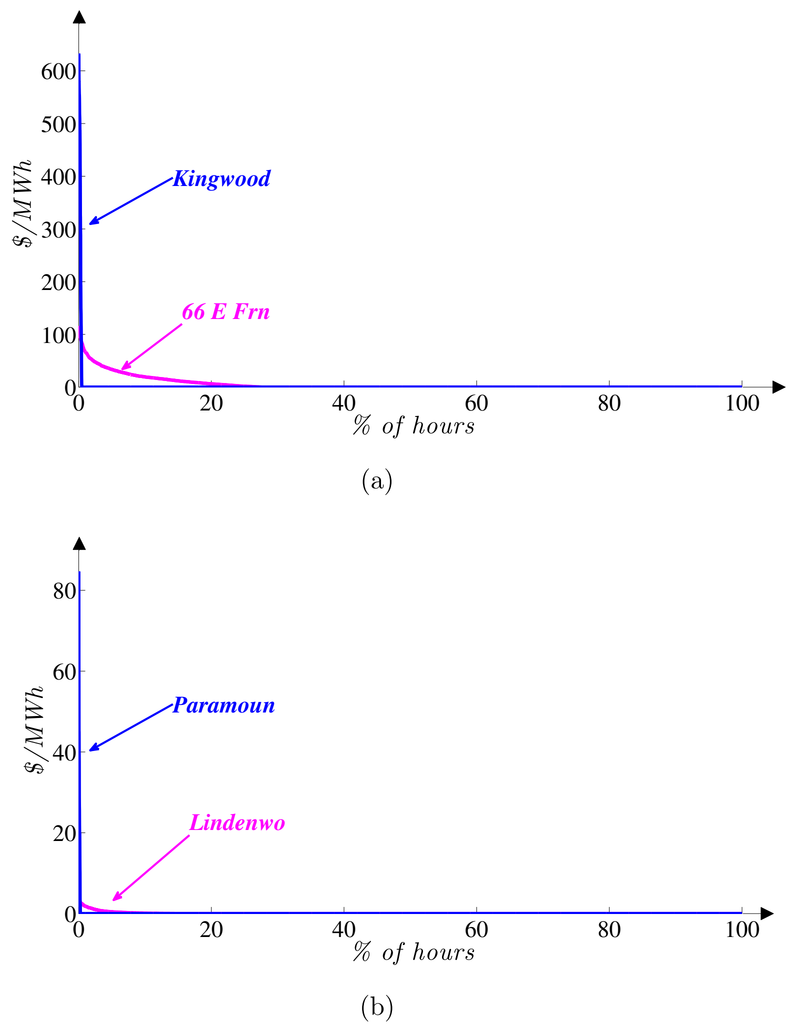

Figure 1.4: $TUCDC$s of 4 selected lines in the PJM ISO network for 2010

distribution factor $LODF$ [22]. Under specified contingency cases involving line outages, the $LODF$s may induce congestion in certain lines that are not outaged. We make extensive use of these insights in casting the portfolio construction problem to be focused on judicious selection of congested lines.

We recast the problem from the LMP differences of node pairs to congested lines. We propose a methodology to solve the speculator's problem where we choose FTR such that the transactions with same node pairs and amounts induce real power flow on the congested lines. However, we cannot do this on all congested lines, because the speculator needs to acquire a large number of FTR and his returns are decreased by the FTR premiums. We judiciously choose a subset of lines and the level of participation on the congested flows on the lines. We use the $TUCDC$ to find the chronic and outage driven constraints and determine the key causal factor of congestion. If we believe that similar events occur in the holding period we identify the lines in the "specified congestion participation" subset. However, there are some lines for which we may not specify the key causal factor of congestion, and their behavior is unknown for the holding period. We choose *FTR* such that such lines are not included in the *FTR* paths. We identify these lines into the "zero congestion participation" subset. In the basis of the two subsets, "specified congestion participation" and "zero congestion participation," we construct the *FTR* portfolio by finding transactions that induce real power flow, according to the level of participation specified by the speculator, on lines in the two subsets. In order to determine the possible node pairs for the transactions, we choose a subset of nodes. This subset includes the terminal nodes of the lines in the two subsets. If we considered all possible node pairs, the computational burden would be large. However, by choosing the terminal nodes of the lines, we know that part of an injection at a *from* or *to* node flows through the line, and that transactions with node pairs from the subset definitely induce flows on the lines in the two subsets. A great number of transactions induce the desired flows on the lines in the two subsets. We choose the solution that provides the minimum number of transactions, since we associate the transactions with *FTR* and we achieve the minimum number of *FTR* in the portfolio. For practical reasons it is very useful to participate in the *FTR* auctions with the minimum number of bids. So, we construct an *FTR* portfolio whose *FTR* have on their paths congested elements; therefore, the associated revenues are non-zero.

1.4 Outline of the Thesis

This thesis consists of four additional chapters and two appendices. In Chapter 2, we review the analytical setting for formulating the speculator's portfolio construction problem. Specifically, we discuss the models deployed in the *FTR* auctions to obtain an understanding of the costs entailed in the portfolio construction. We also examine the modeling and formulation of the *DAM* clearing problem so as to understand the nature of the revenue stream. In addition, we recast the statement of the *IGO* market clearing problem to gain valuable insights into the key drivers of congestion rents collected by the

IGO and reimbursements to the *FTR* holders. We provide in this chapter the key tools and insights we use in the development of the solution approach to the *FTR* portfolio construction problem faced by the speculator.

In Chapter 3 we provide the steps of the approach developed to construct the *FTR* portfolio. We describe the input parameters and how we transform the speculator's problem by focusing on two subsets of lines and their transmission usage costs instead of the *LMP* differences of node pairs. We determine the *FTR* specifications by finding transactions that induce on the lines in the subsets the desired flows. However, there is a large number of node pairs that could be taken into consideration. We exploit the physical characteristics of the systems and choose a subset of nodes. The main concept is the identification of injection and withdrawal nodes with the property that part of the transaction flows through the lines in the two subsets. We construct an optimization problem with the objective function of minimizing the number of transactions such that they induce the desired flows on the lines in the two subsets. We associate each transaction with an *FTR* and construct the *FTR* portfolio with minimum number of node pairs.

In Chapter 4, we describe the subset of representative numerical results we obtained using the proposed approach. The results are on three test systems of different scales: a 30-bus test system, the *IEEE* 118-bus network and the *PJM* grid. We use the small system to indicate the mechanics of the approach and to understand the capability of the scheme. For the 118-bus system, we provide a set of sensitivity studies to test the robustness of the approach. For the *PJM ISO* network, we show the effectiveness of the approach for a large-scale system. In our discussions, we provide insights into the results and interpret them to give the reader a physical intuition for the nature of the problem.

We provide in Chapter 5 a summary of the key contributions of the work presented in this thesis. We also indicate directions for future research in the topic. The thesis has four additional appendices. In Appendix A, we present mathematical formulation of the *FTR* auction. In Appendix B, we give the proof of the lemma used in Chapter 3 to construct the portfolio. The lemma concerns the fact that the topological characteristics of the system limit the number of lines on which we may specify the flows. In Appendix C, we give a picture of the network topology of the *IEEE* 118-bus system and in D, we provide the data used in the application studies of Chapter 4

CHAPTER 2

MODELING ASPECTS IN *FTR* ANALYSIS

In this chapter, we review the modeling aspects that we make detailed use of in developing the solution approach to the speculator's problem. We start out with a discussion of the modeling issues that formulate the FTR acquisition and revenues in terms of the LMP differences. We then recast the formulation of the optimal power flow (OPF) problem used in the clearing of the DAMs as well as in congestion management, to focus on the key role played by the congested lines in the determination of the market outcomes. The recast formulation allows the expression of the revenues of the speculator for the FTR holdings in terms of the transmission usage costs of the congested lines. The insights provided by the reformulation constitute a basic building block of the approach.

2.1 Modeling Issues

We use the framework developed by M. Liu and G. Gross for the modeling of congestion effects and FTR evaluations [23]. This framework has the capability to allow the analysis of a broad range of problems associated with ensuring price certainty for transmission services and provides the flexibility to analyze issues and design structures for the provision of transmission services in the competitive environment. The framework includes the description of the financial markets and the DAMs. In order to present the formulation of the clearing mechanisms of the FTR auction and the DAM, we need to describe the physical network. However, the network may change in every hour h of the DAMs and therefore we represent 24 different snapshots for the hourly DAMs. We use a "representative" network to clear the auction for FTR and we use a single snapshot for that network for the entire duration of the FTR holding period.

We consider a power system consisting of the set of $(N+1)$ nodes $\mathscr{N} = \{0, 1, \ldots, N\}$, with the slack bus at node 0, and the set of L lines $\mathscr{L} = \{\ell_1, \ldots, \ell_L\}$. We denote each line by the ordered pair $\ell = (n, m)$ where n is the *from* node, and m is the *to* node with $n, m \in \mathscr{N}$, with the real power flow $f_\ell \geq 0$ whenever the flow is from n to m and $f_\ell < 0$ otherwise. We assume that each bus is connected to at least one other bus. We consider a *lossless* network with the diagonal branch susceptance matrix $\underline{\boldsymbol{B}}_d \in \mathbb{R}^{L \times L}$. Let $\underline{\boldsymbol{A}} \in \mathbb{R}^{L \times N}$ be the reduced branch-to-node incidence matrix for the subset of nodes $\mathscr{N}/\{0\}$ and $\underline{\boldsymbol{B}} \in \mathbb{R}^{N \times N}$ be the corresponding nodal susceptance matrix. We assume the network contains no phase shifting devices and so $\underline{\boldsymbol{B}}^T = \underline{\boldsymbol{B}}$. We denote the slack bus nodal susceptance vector by $\underline{\boldsymbol{b}}_0 = [b_{01}, \ldots, b_{0N}]^T$, with

$$\underline{\boldsymbol{b}}_0 + \underline{\boldsymbol{B}}\,\underline{\boldsymbol{1}}^N = \underline{\boldsymbol{0}} \ ,$$

where $\underline{\boldsymbol{1}}^N$ is the unit N-dimensional vector.

We use the network description to formulate the primary *FTR* auction for *FTR* contracts. The *FTR* auction clearing mechanism is formulated by considering a "representative" network topology for the entire *FTR* holding period and by taking into account a list of contingencies. In the *FTR* auction model, the transmission constraints for the base case and the single-line outage contingency cases are expressed in terms of the power (*PTDF*s) and outage (*OTDF*s) transfer distribution factors respectively [24]. The auction clearing mechanism is the same for long-term, annual, monthly auctions but the offered transmission capability changes accordingly. We formulate the auctions in a way that may be modified to describe the characteristics of all auctions. We consider the *FTR* auction consisting of a set of $\mathbb{B}$ buyers and the *IGO* as the only seller. Each bid consists of $\{\overline{\Gamma}, \overline{c}\}$, where $\overline{\Gamma} = \{i, j, \overline{\gamma}\}$ is the desired *FTR*, with i the injection node, j the withdrawal node, $\overline{\gamma}$ the desired amount to buy, and $\overline{c}$ the willingness to pay. A buyer's b k bid for *FTR* is represented by $\left\{\overline{\Gamma}_k^{(b)}, \overline{c}_k^{(b)}\right\}$, where $\overline{\Gamma}_k^{(b)} = \{i_k^{(b)}, j_k^{(b)}, \overline{\gamma}_k^{(b)}\}$, $k = 1, \ldots K^{(b)}$. The clearing of the *FTR* auction is determined by solving an optimization problem, where the desired *FTR* are represented by actual transactions. The objective of the optimization problem is to maximize the bid-based value of *FTR*, with all the physical constraints not violated. An analytical formulation of the *FTR* auction clearing mechanism is given in Appendix A. The outcomes of the *FTR* auctions are the actual *FTR* amounts bought

$\gamma_k^{(b)},\ k = 1, \ldots, K^{(b)},\ b = 1, \ldots, \mathcal{B}$ and the dual variables β_ℓ^M and β_ℓ^m of the real power flow constraints for each line ℓ. The actual amount for *FTR* $\Gamma_k^{(b)}$ is $\gamma_k^{(b)}$ and the premium price is

$$c_k^{(b)} = \sum_{\ell \in \tilde{\mathscr{L}}} \phi_\ell^{\{i_k^{(b)}, j_k^{(b)}\}} (\beta_\ell^M - \beta_\ell^m) \ , \tag{2.1}$$

where $\tilde{\mathscr{L}} = \left\{ \ell_i \ : \ i \ \in \{1, \ldots, L\},\ \beta_{\ell_i}^M > 0 \text{ or } \beta_{\ell_i}^m > 0 \right\}$. The winning bid representation of the k^{th} *FTR* of buyer b is

$$\Gamma_k^{(b)} = \{ i_k^{(b)}, j_k^{(b)}, \gamma_k^{(b)} \} \ . \tag{2.2}$$

The *FTR* premiums and actual amounts are determined by the outcomes of the *FTR* auction. The *FTR* revenues depend on the outcomes of the *DAM*s. We formulate the *DAM* clearing mechanism. The state variable of the voltage phase angle at bus n is θ_n, the n^{th} element of $\underline{\boldsymbol{\theta}} \in \mathbb{R}^N$. We state the real power flow equations of the network and use p_n^e (p_n^x) as the power injection (withdrawal) at each $n \in \mathscr{N}$ and construct the N-vectors

$$\begin{aligned} \underline{\boldsymbol{p}}^e &= [p_1^e, \ldots, p_N^e]^T \\ \underline{\boldsymbol{p}}^x &= [p_1^x, \ldots, p_N^x]^T \ . \end{aligned}$$

The state variable $\underline{\boldsymbol{\theta}}$ is determined by the equations

$$\underline{\boldsymbol{p}}^e - \underline{\boldsymbol{p}}^x = \underline{\boldsymbol{B}}\, \underline{\boldsymbol{\theta}} \tag{2.3}$$

$$p_0^{in} - p_0^{out} = \underline{\boldsymbol{b}}_0^T\, \underline{\boldsymbol{\theta}} \tag{2.4}$$

The vector in $\mathbb{R}^L$ of the real power flows on the lines of the network

$$\underline{\boldsymbol{f}} = \underline{\boldsymbol{B}}_d\, \underline{\boldsymbol{A}}\, \underline{\boldsymbol{\theta}} = [f_{\ell_1}, \ldots, f_{\ell_L}]^T \, . \tag{2.5}$$

The constraints on the real power flows are represented through the following inequalities:

$$\begin{aligned} \underline{\boldsymbol{f}} &\leq \underline{\boldsymbol{f}}^M \\ \underline{\boldsymbol{f}} &\geq -\underline{\boldsymbol{f}}^m \ , \end{aligned}$$

where

$$\underline{\boldsymbol{f}}^M = [f^M_{\ell_1}, \ldots, f^M_{\ell_L}]^T$$
$$\underline{\boldsymbol{f}}^m = [f^m_{\ell_1}, \ldots, f^m_{\ell_L}]^T ,$$

the values of the maximum real power flow allowed through the lines in $\mathscr{L}$ in the same direction and in the opposite direction of line ℓ respectively. A line ℓ is congested if the real flow through the line equals one of the line flow limits, i.e., $f_\ell = f^M_\ell$ either $f_\ell = -f^m_\ell$.

We state the hour h *DAM* problem for the set of S sellers $\mathscr{S} \triangleq \{s_1, \ldots, s_S\}$ and the set of B buyers $\mathscr{B} \triangleq \{b_1, \ldots, b_B\}$. The objective of these market players is to maximize the societal net benefits given by the difference between the benefits $\sum_{j=1}^{B} \beta^{b_j}(p^{b_j})$ of the buyers and the costs $\sum_{i=1}^{S} \kappa^{s_i}(p^{s_i})$ to purchase from the sellers. The power injection (withdrawal) p^{in}_n (p^{out}_n) at each $n \in \mathscr{N}$ is given by

$$p^e_n = \sum_{\substack{s_i \in \mathscr{S} \text{ is} \\ \text{at node } n}} p^{s_i} \text{ and } p^x_n = \sum_{\substack{b_j \in \mathscr{B} \text{ is} \\ \text{at node } n}} p^{b_j} .$$

The hour h *DAM* optimization problem statement is

$$\begin{array}{lll} \max & \left\{ \sum_{j=1}^{B} \beta^{b_j}(p^{b_j}) - \sum_{i=1}^{S} \kappa^{s_i}(p^{s_i}) \right\} & \\ \text{subject to} & \underline{\boldsymbol{p}}^e - \underline{\boldsymbol{p}}^x = \underline{\boldsymbol{B}}\,\underline{\boldsymbol{\theta}} & \longleftrightarrow \quad \underline{\boldsymbol{\lambda}} \\ & p^e_0 - p^x_0 = \underline{\boldsymbol{b}}^T_0\,\underline{\boldsymbol{\theta}} & \longleftrightarrow \quad \lambda_0 \\ & \underline{\boldsymbol{f}} = \underline{\boldsymbol{B}}_d\,\underline{\boldsymbol{A}}\,\underline{\boldsymbol{\theta}} \leq \underline{\boldsymbol{f}}^M & \longleftrightarrow \quad \underline{\boldsymbol{\mu}}^M \\ & -\underline{\boldsymbol{f}} \leq \underline{\boldsymbol{f}}^m & \longleftrightarrow \quad \underline{\boldsymbol{\mu}}^m \end{array} \tag{2.6}$$

We clearly indicate in (2.6) the dual variables corresponding to the various constraints.

In order to determine the total revenues for hour h of the *FTR* portfolio

$$\mathscr{F} \triangleq \{\Gamma_1, \ldots, \Gamma_K\}, \tag{2.7}$$

where $\Gamma_k = \{i_k, j_k, \gamma_k\}$ with holding period $\mathscr{T} = \{h_{start}, \ldots, h_{end}\}$, we use the *DAM* outcomes for hour h and compute the difference between the source and sink node *LMP*s, so as to determine the *FTR* revenues for $\mathscr{F}$.

$$\eta\big|_h = \sum_{\Gamma_k \in \mathscr{F}} \left(\lambda_{j_k}\big|_h - \lambda_{i_k}\big|_h\right) \gamma_k \ . \tag{2.8}$$

The total revenues for the entire holding period of portfolio $\mathscr{F}$ are

$$\eta = \sum_{h \in \mathscr{T}} \eta\big|_h \ . \tag{2.9}$$

In this section, we discussed the modeling aspects of the speculator's problem. We described analytically the environment the speculator participates in to acquire *FTR* and the *DAM* that determines the *FTR* revenues. The revenues are a function of the *LMP* difference of the *FTR* node pairs. The high volatility of *LMP* differences and the large combination of possible *FTR* node pairs makes the speculator's problem difficult to manage. Thus, we use the *DAM* clearing mechanism formulation to recast the speculator's problem into an easier to handle form, based on the insights we gain in the next section.

2.2 Analysis of the *DAM* Clearing Model

We use the salient characteristics of power systems to recast the speculator's problem into a more manageable form. An *LMP* difference between two nodes signals that one or more line flows have reached their maximum limit; i.e., one or more transmission constraints is binding. There is an associated dual variable with each constraint, which may be interpreted as the cost to relieve each constraint. The dual variables of the transmission constraints are indicated in (2.6) as $\underline{\boldsymbol{\mu}}^M$ and $\underline{\boldsymbol{\mu}}^m$. We denote by $\underline{\boldsymbol{\mu}} = \underline{\boldsymbol{\mu}}^M - \underline{\boldsymbol{\mu}}^m$ the transmission usage cost vector for the L lines. Lines that are not congested have a zero contribution in the *LMP* differences, since their transmission usage cost is zero.

In order to derive the relationship between the *LMP* differences of node pairs and the dual variables of the transmission constraints, we use the Lagrangian

$$\mathcal{L}\big(\underline{\boldsymbol{p}}^{e}, \underline{\boldsymbol{p}}^{x}, p_{0}^{in}, p_{0}^{out}, \underline{\boldsymbol{\theta}}, \underline{\boldsymbol{\lambda}}, \lambda_{0}, \underline{\boldsymbol{\mu}}^{M}, \underline{\boldsymbol{\mu}}^{m}\big) = \sum_{j=1}^{B} \beta^{b_j}(p^{b_j}) - \sum_{i=1}^{S} \kappa^{s_i}(p^{s_i}) +$$
$$\underline{\boldsymbol{\lambda}}^{T}\left(\underline{\boldsymbol{p}}^{e} - \underline{\boldsymbol{p}}^{x} - \underline{\boldsymbol{B}}\,\underline{\boldsymbol{\theta}}\right) + \lambda_{0}\big(p_{0}^{e} - p_{0}^{x} - \underline{\boldsymbol{b}}_{0}^{T}\,\underline{\boldsymbol{\theta}}\big) +$$
$$(\underline{\boldsymbol{\mu}}^{M})^{T}\big(\underline{\boldsymbol{f}}^{M} - \underline{\boldsymbol{B}}_{d}\,\underline{\boldsymbol{A}}\,\underline{\boldsymbol{\theta}}\big) + (\underline{\boldsymbol{\mu}}^{m})^{T}\big(\underline{\boldsymbol{f}}^{m} + \underline{\boldsymbol{B}}_{d}\,\underline{\boldsymbol{A}}\,\underline{\boldsymbol{\theta}}\big)\ . \tag{2.10}$$

The stationarity conditions are given by

$$\frac{\partial \mathcal{L}}{\partial \underline{\boldsymbol{\theta}}} = -\underline{\boldsymbol{B}}^{T}\,\underline{\boldsymbol{\lambda}} - \underline{\boldsymbol{b}}_{0}\,\lambda_{0} - \underline{\boldsymbol{A}}^{T}\,\underline{\boldsymbol{B}}_{d}\,\underline{\boldsymbol{\mu}} = \underline{\boldsymbol{0}}\ . \tag{2.11}$$

We use the *ISF* matrix $\underline{\boldsymbol{\Psi}}$ to restate the relationship linking the $\underline{\boldsymbol{\lambda}}, \lambda_{0}$ and $\underline{\boldsymbol{\mu}}$, as

$$\underline{\boldsymbol{\lambda}} = \lambda_{0}\,\underline{\mathbf{1}}^{N} - \underline{\boldsymbol{\Psi}}^{T}\,\underline{\boldsymbol{\mu}}\ , \tag{2.12}$$

and refer to $\lambda_{n},\ n = 0, 1, \ldots, N,$ as the *LMP* at node n and to $\underline{\boldsymbol{\mu}} = [\mu_{\ell_1}, \ldots, \mu_{\ell_L}]^{T}$ as the transmission usage cost vector. It follows that

$$\lambda_{n} = \lambda_{0} - \sum_{\ell \in \mathscr{L}} \psi_{\ell}^{n}\,\mu_{\ell}\,, \quad \forall\, n \in \mathscr{N}/\{0\}. \tag{2.13}$$

We interpret physically the relationship in (2.13) by considering an injection at node n and its withdrawal at node n'. We interpret $\phi_{\ell}^{\{n,n'\}}$ as the fraction of the transaction with node pair $\{n, n'\}$ of $1\,MW$ that flows on the line ℓ. We rewrite (2.13) in terms of the *PTDF*s so that

$$\lambda_{n'} - \lambda_{n} = \sum_{\ell \in \mathscr{L}} \phi_{\ell}^{\{n,n'\}}\,\mu_{\ell}\ . \tag{2.14}$$

We next make use of the complementary slackness conditions of the optimization problem (2.6). Clearly, $\mu_{\ell} = 0$ for any line ℓ whose flow is not at its limits. We define the subset $\tilde{\mathscr{L}} = \big\{\ell_i : i \in \{1, \ldots, L\},\ \mu_{\ell_i} \neq 0\big\}$ to be

$$\lambda_{n'} - \lambda_{n} = \sum_{\ell \in \tilde{\mathscr{L}}} \phi_{\ell}^{\{n,n'\}}\,\mu_{\ell}\ . \tag{2.15}$$

In order to bring out the implications of the complementary slackness conditions for every hour h, we represent explicitly in the equations that follow the explicit dependence over hour h, as the results may vary from hour to hour. In particular, the market outcomes for hour h, denoted by $\big|_h$, obtain of the *FTR* revenues for $\Gamma = \{i, j, \gamma\}$:

$$\eta\big|_h = \left(\lambda_j\big|_h - \lambda_i\big|_h\right)\gamma = \sum_{\ell \in \tilde{\mathscr{L}}\big|_h} \mu_\ell\big|_h \phi_\ell^{\{i,j\}}\Big|_h \gamma \ . \tag{2.16}$$

For an injection γ at node i and withdrawal γ at node j we approximate the change Δf_ℓ in the flow on line ℓ by the *PTDF* of line ℓ times the amount γ:

$$\eta\big|_h = \sum_{\ell \in \tilde{\mathscr{L}}\big|_h} \mu_\ell\big|_h \Delta f_\ell\big|_h \ . \tag{2.17}$$

Clearly, (2.17) indicates that only the congested lines contribute to the hour h revenues. We conclude, therefore, that for each hour $h \in \mathscr{T}$, the revenues $\eta\big|_h$ are purely a function of the transmission usage costs of the congested lines $\ell \in \tilde{\mathscr{L}}\big|_h$.

We therefore focus on a portfolio construction strategy that allows the speculator to include *FTR* node pairs with paths that have congested lines. More specifically, the hourly revenues depend on the flows $\Delta f_\ell\big|_h$ that transactions, with same node pairs and amounts as *FTR*, induce on the congested lines. We may view the flows as a weighting factor of the transmission usage cost of each congested line. Our decision variables in the *FTR* selection are the source and sink nodes and the *FTR MW* amounts. Therefore, we use the relationships (2.14)-(2.16) to translate backwards, from a specified flows amount on a congested line to the transaction amount γ that sets up $\Delta f_\ell\big|_h$ for every hour h. We use this insight as the key building block in the construction of the *FTR* portfolio for the speculator problem.

In this chapter, we discussed the modeling issues of the *FTR* environment. We determined the *FTR* acquisition cost in (2.1) and the *FTR* revenues that depend on the outcomes of the *DAM*s over the holding period (2.6) in terms of the *LMP* differences. We recast the *OPF* formulation of the *DAM* and found a relationship between the *LMP* difference of a node pair and the transmission usage costs of the congested lines (2.14). This insight is a key element of the construction of the *FTR* portfolio. By using (2.14), we express the *FTR* revenues in terms of the transmission usage costs of the congested lines (2.16). We use the insights of this chapter to recast the speculator's problem and construct the *FTR* portfolio.

CHAPTER 3

OPTIMIZED *FTR* PORTFOLIO CONSTRUCTION

We devote this chapter to the detailed analysis of the *FTR* portfolio construction for the speculator problem. We start out with the qualitative statement of the problem and introduce necessary assumptions to formulate a mathematical statement. We describe the input data that the speculator provides in the *FTR* portfolio construction model, i.e., his requirements. Instead, of looking at the *LMP* differences of node pairs, we base the *FTR* portfolio construction on set of congested lines. In particular, the speculator identifies the lines into two subsets, the "specified congestion participation" and "zero congestion participation". We specify the *FTR* that have on their paths the lines identified by the speculator. In order to determine the *FTR* node pairs, we choose a subset of nodes to make the proposed methodology computationally efficient. We construct the optimized *FTR* portfolio by choosing the minimum number of node pairs that satisfy the speculator's requirements.

3.1 Qualitative Problem Formulations and Assumptions

A speculator participates in *FTR* auctions to acquire *FTR*, in order to have returns that are as good as possible. A variety of *FTR* products is offered in the auctions. We focus on solving the portfolio construction problem for a simplified form where we consider the acquisition in a single auction and the purchase of *FTR* contracts for a specified holding period. Moreover, we do not consider any other *FTR* holdings of the speculator. We denote the *FTR* with source (sink) node i (j) in the MW amount γ by the triplet

$$\varGamma = \{i, j, \gamma\} \ . \tag{3.1}$$

The speculator's problem concerns the identification of the elements of the optimized *FTR* portfolio $\mathscr{F}$, where

$$\mathscr{F} \triangleq \{\varGamma_1, \ldots, \varGamma_K\} . \tag{3.2}$$

For each $\varGamma_k \in \mathscr{F}$, we need to specify the triplet elements i_k, j_k and γ_k, where $k = 1, \ldots, K$. We develop the proposed approach assuming that the network is connected, lossless and has no phase-shifting devices.

We use the insights derived in Section 2.2 and no longer base the *FTR* selection on the *LMP* differences of node pairs. Instead, we focus on the transmission usage costs of lines to construct the *FTR* portfolio. We focus on a portfolio construction strategy that allows the speculator to include *FTR* node pairs with paths that have congested lines. Conceptually, *FTR* revenues depend on the real power flow that transactions with same node pairs and *MW* amounts as *FTR* induce on the congested lines of the system and their transmission usage costs. However, the speculator needs to purchase too large a number of *FTR* to include all congested lines on the paths of *FTR* in the portfolio for every hour of the holding period and the *FTR* premiums reduce his returns. Thus, the identification of a subset of congested lines is a key step in the construction methodology. From a study of historical data, a subset of lines that, from past behavior, get congested may be identified. Moreover, we use the topological characteristics of the underlying network to choose lines that get congested in the *FTR* holding period.

3.2 Mathematical Statement and Input Data Requirements

We recast the speculator's problem by using the insights derived in Section 2.2 and focus on the transmission usage costs of the congested lines. The speculator chooses *FTR* such that transactions with the same node pairs and amounts induce real power flow on the congested direction of the lines. However, the speculator cannot do this for all lines and therefore needs to identify a subset of congested lines. We make use of the historical data and topological characteristics, as described in Section 1.3, to focus on a subset of congested elements.

We use the *TUCDC* to neglect the lines that have a small impact on the *FTR* revenues, because they get congested for only a few hours of the holding period or their transmission usage costs do not exceed the price threshold. Next, we identify the key causal factor of congestion, and we may use offer and bid forecasts and maintenance schedules to be able to predict which transmission constraints will more likely bind, under the assumption that the future is going to be a continuation of the past. We may specify the subset of lines that will likely get congested, which we call "specified congestion participation " subset. However, there exist some lines for which we may not specify a key causal factor of congestion. This is due to the fact that the lines are affected by various factors and in such cases we are not in a position to predict their behavior in the holding period. We identify lines with unknown behavior as the "zero congestion participation" subset, such that the transactions with same node pairs and amount as *FTR* in the portfolio induce zero flow on these lines and, therefore, the *FTR* revenues are influenced by the transmission usage costs of lines in this subset. The network topology imposes constraints on the ability to specify the flows on all lines. In fact, the line flow restriction lemma, whose statement and proof are given in Appendix B, provides an exact bound on the number of lines whose flows may be specified. We make use of that lemma in the statement of the problem and consequently in the input data requirements. Because they do not get congested, the remaining lines form the "do-not-care congestion participation" subset, which gives us flexibility in determining the node pairs and amounts of the *FTR*. When we specify for the entire set of lines the speculator's participation, we may end up with an unsolvable problem, since there is a limit on the number of lines over which we may specify the flows due to purely topological considerations (Appendix B). Even if we specify the speculator's participation so as to have a feasible system, we over-constrain our problem by specifying the flows on lines that are not congested in the *FTR* holding period and, therefore, do not affect the *FTR* revenues. By focusing only on the two subsets, specified congestion participation and zero congestion participation, we augment the feasible region. The speculator specifies his requirements by the quadruplets

$$\zeta = \left\{ \delta, \ell, z, \mathscr{L}^{[c]} \right\} . \tag{3.3}$$

For a particular line ℓ, the element δ indicates the subset to which the line ℓ belongs: for $\delta = 1$ line ℓ belongs in the specified congestion participation subset and his level of participation is z MW under the contingency case $\mathscr{L}^{[c]}$, where $\mathscr{L}^{[c]} = \{\text{lines that are outaged}\}$ or $\mathscr{L}^{[c]} = \{\varnothing\}$ in the base case topology, and for $\delta = 0$ the line belongs to the zero congestion participation subset with $z = 0$.

We make concrete the concepts of the two subsets, specified congestion participation and zero congestion participation, by the illustrative example of a 10-bus system, whose one line diagram is shown in Fig. 3.1. Based on

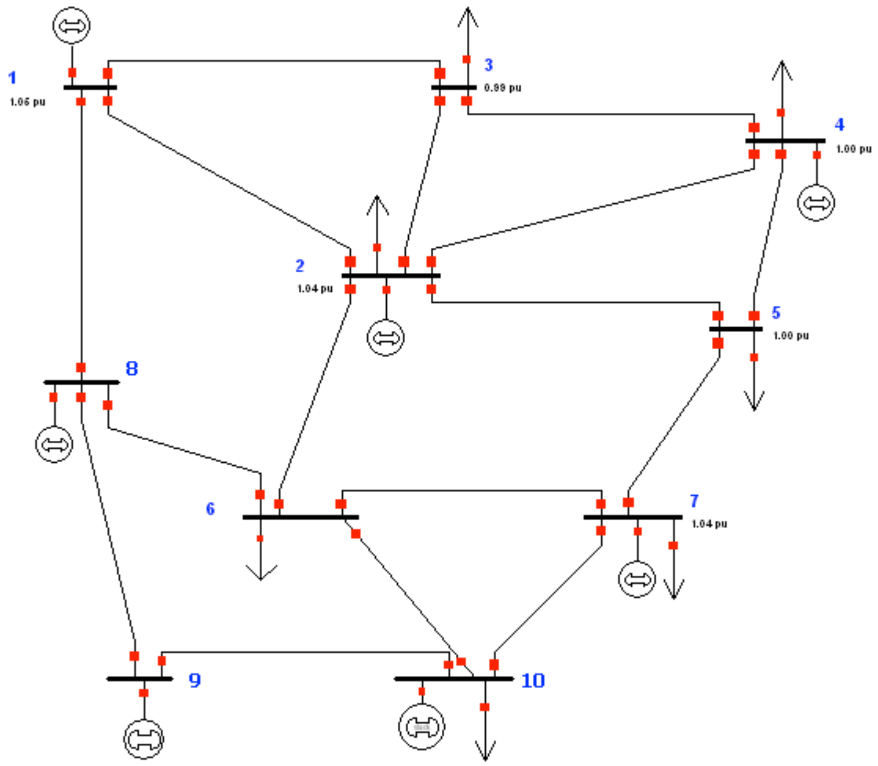

Figure 3.1: Network topology of the 10-bus system

topological considerations, discussed in Appendix B, the maximum number of lines we may arbitrarily specify for the speculator's participation is 9. The fact that different lines get congested for different topological conditions is illustrated in a 10-bus system by looking at two snapshots corresponding to the base case and a specific contingency case. The snapshot of hour h provides the base case, with all lines in service, and that of hour h' corresponds to the snapshot when line $(1, 2)$ is outaged. The resulting flows are given in Fig. 3.2. We base the identification of the two subsets on the two snapshots of the system. At hour h the only line that is congested is line $(7,5)$ in direction from 7 to 5. However, at hour h', which is depicted in Fig. 3.2b, where line $(1,2)$ is outaged, lines $(1,3)$ and $(7,5)$ are congested. Line $(7,5)$ is now congested in the opposite direction than that of hour h. We identify line $(7,5)$ in the zero congestion participation subset, since the key causal factor of congestion may not be identified and the transmission usage costs of the lines might negatively influence the revenues if it is included in the *FTR* paths. However, we may determine the key causal factor of congestion for line $(1,3)$, since it gets congested due to the line outage of line $(1,2)$. We identify line $(1,3)$ in the specified congestion participation subset.

On the basis of the two subsets, specified congestion participation and zero congestion participation, we construct the *FTR* portfolio by finding transactions that induce real power flow, according to the level of participation specified by the speculator, on lines in the two subsets. We specify

$$\begin{aligned} & \mathscr{F} = \left\{ \mathit{\Gamma}_1, \mathit{\Gamma}_2, \ldots, \mathit{\Gamma}_K \right\} \\ \text{subject to} \quad & \text{for } \delta = \mathit{0}\text{: line } \ell \text{ is on their path and} \\ & \text{the participation level is } z \text{ in topology } \mathscr{L}^{[c]} \\ & \text{for } \delta = 1\text{: line } \ell \text{ is on their path} \\ & \text{but with zero participation in topology } \mathscr{L}^{[c]} \end{aligned} \tag{3.4}$$

We discuss the method analytically in Section 3.3.

3.3 Solution Approach

We explicitly use the insights derived in Section 2.2 and determine the *FTR* in the portfolio by determining transactions, which we associate with each *FTR*. We wish to specify transactions that satisfy the speculator's requirements, i.e., to induce the desired level of participation on the lines in the two subsets in the desired topologies. Let a transaction $\underline{\boldsymbol{w}}$ be specified by the vector

$$\underline{\boldsymbol{w}} = [m, n, a]^T \ , \tag{3.5}$$

where m is the *from* node, n is the *to* node and a is the *MW* amount. We propose a practical approach for a speculator to determine the num-

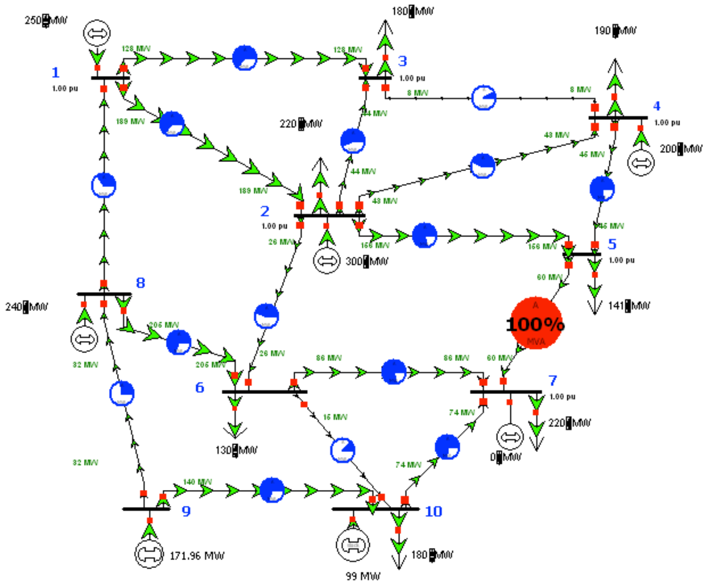

(a)

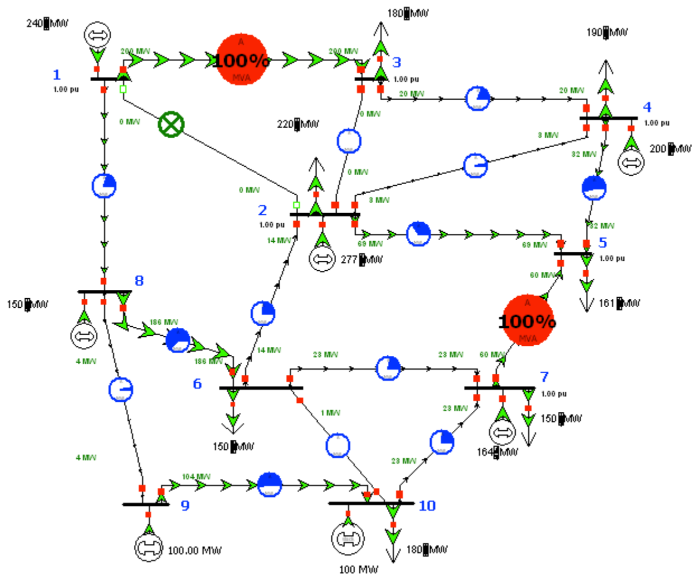

(b)

Figure 3.2: The subset of congested lines for (a) base case in hour h and (b) the contingency case of line $(1, 2)$ outage in hour h' of the 10-bus system

ber of transactions U and specify them once he has the V specifications $\zeta^1, \zeta^2, \ldots, \zeta^V$. Conceptually, the idea is to determine the number of transactions U and the components of $\underline{\boldsymbol{w}}_u = [m_u, n_u, a_u]^T$, $u = 1, \ldots, U$. These components must be selected in such a way that they satisfy the V specifications $\zeta^1, \zeta^2, \ldots, \zeta^V$. The determination of the node pairs $\{m_u, n_u\}$ is too large a problem if we consider all the possible nodes pairs in $\mathscr{N}$, since the number is of the order of $\binom{N+1}{2}$. Taking into consideration the large-scale nature of today's grid, we can easily see that the problem becomes extremely big and computationally burdensome. We may select, however, a subset of the network nodes by taking into consideration the physical characteristics of the system. We choose the terminal nodes of the lines in the specified congestion participation and zero congestion participation subsets, since we know that part of an injection at a *from* or *to* node flows through the line, and that transactions with node pairs from the subset definitely induce flows on the lines in the two subsets. Since we associate a *from* node and a *to* node for a line ℓ, we limit our interest to the subset of nodes that are associated with the lines in the two subsets.

$$\mathscr{H} = \Big\{ g : g \text{ is either a } \textit{from} \text{ or a } \textit{to} \text{ node of line } \ell \text{ in the specification } \zeta^{v},\ v = 1, \ldots, V \Big\}. \tag{3.6}$$

As H, the cardinality of $\mathscr{H}$, is considerably smaller than $\binom{N+1}{2}$, we reduce the size of the computational burden to construct the pairs for possible transactions. With the example of a 10-bus system in Fig. 3.1, we demonstrate that an injection or withdrawal at a *from* or *to* node of a line has an effect on the line flow. We calculate the *ISF*s of all nodes for all the lines in the system, with slack node 1. We order the *ISF*s by their absolute value in Table 3.1. The ordering makes sense for lines that do not include node 1 as either a *from* or a *to* node. We present the results for 4 lines and notice that their *from* and *to* nodes are in the first 3 positions. So, it makes sense to

Table 3.1: Nodes ordered according to the absolute value of the *ISF*, with respect to each line

line	**ordered nodes**		
(2,4)	4	3	2
(3,4)	4	3	5
(4,5)	5	7	4
(10,7)	10	7	9

choose the terminal nodes of lines in the specified congestion participation and zero congestion participation subsets. We form the set $\mathscr{U}$ of ordered pairs of nodes in $\mathscr{H}$ with

$$\mathscr{U} = \Big\{ \{m, n\} : m, n \in \mathscr{H}, m < n \Big\} . \tag{3.7}$$

The cardinality U of $\mathscr{U}$ is given by $U = \binom{H}{2}$. At this point, the pairs of possible transactions are given by $\{m_u, n_u\} \in \mathscr{U}$, for $u = 1, \ldots, U$. However, a transaction is specified by the vector $\underline{\boldsymbol{w}}_u = [m_u, n_u, a_u]^T$. So, we need to determine the amounts a_u for $u = 1, \ldots, U$. If the solution produces $a_u < 0$ for some $u \in \{1, \ldots, U\}$, we replace the transaction $\underline{\boldsymbol{w}}_u = [m_u, n_u, a_u]^T$ by $\underline{\boldsymbol{w}}_u{}' = [n_u, m_u, -a_u]^T$; i.e, we interchange the withdrawal and injection nodes, and the amount is set to the negative value of a_u, since a transaction amount must be a positive quantity.

The determination of the amounts a_u is obtained by writing an equation for each ζ^v, to be able to specify the transactions w_u. For each $v = 1, \ldots, V$, the transactions must induce flow z^v in line ℓ in the contingency case $\mathscr{L}^{[c]}$ specified by ζ^v. Usually, the topology refers to a representative topology of the system, i.e., the base case, for the period under consideration, in the same notion as in *FTR* auctions. However, in the cases where a line in one of the subsets gets congested due to another line outage, then the network topology changes. We formulate the solution for any possible topology. If the topologies that are included in the quadruplets refer to the representative case and the single line outage cases, we may simplify the problem by using the *PTDF*s and the *OTDF*s of the representative topology. The effect that a transaction has on a line can be approximated by its *PTDF* for the specified topology. The real power flow on line ℓ' due to a transaction $\underline{\boldsymbol{w}} = [m, n, a]^T$ is approximated by $\big(\phi_{\ell'}^{\{m,n\}}\big)^{[c]} a$. The total flow in line ℓ' is approximated by the sum of the products of the appropriate *PTDF* and the transaction amount. Therefore, each specification $\zeta_v,\ v = 1, \ldots, V$ of the speculator may be represented by

$$\left[\left(\phi_{\ell}^{\{m_1,n_1\}}\right)^{[c]} \quad \ldots \quad \left(\phi_{\ell}^{\{m_u,n_u\}}\right)^{[c]} \right] \begin{bmatrix} a_1 \\ \vdots \\ a_u \end{bmatrix} = z^v \quad \text{or} \quad \underline{\tilde{\boldsymbol{\Phi}}}\, \underline{\boldsymbol{a}} = \underline{\boldsymbol{z}} \ , \tag{3.8}$$

where row v of $\underline{\tilde{\boldsymbol{\Phi}}}$ is constructed from the *PTDF*s of the network topologies specified in each quadruplet ζ^v. We determine the amounts a_u of the U

transactions by solving (3.8). We notice that

$$rank\left(\underline{\tilde{\boldsymbol{\Phi}}}\right) = rank\left(\left[\underline{\tilde{\boldsymbol{\Phi}}} \vdots \underline{\boldsymbol{z}}\right]\right) , \tag{3.9}$$

since the number of lines in both subsets does not exceed the number of nodes in the system and the lines do not form a loop, so there exist transactions that have the desired effects on the lines. Furthermore, we see that

$$rank\left(\underline{\tilde{\boldsymbol{\Phi}}}\right) < U . \tag{3.10}$$

The dimension of the matrix $\underline{\tilde{\boldsymbol{\Phi}}}$ is $H \times U$. However $U = \binom{H}{2}$ and U is always greater than H for $H > 3$. We assume that $H > 3$ because H is the cardinality of the set $\mathscr{H}$, and if the specifications ζ are greater than or equal to two, then H is greater than 3. We know that the rank of a matrix may not exceed the minimum number of either rows or columns, so we may conclude that the system of equations in (3.8) is underdetermined.

There is a need to have additional criteria to ensure a unique solution. We formulate the optimization problem of minimizing the p-norm of the vector $\underline{\boldsymbol{a}}$ subject to the constraints described by the system (3.8).

$$\begin{aligned} &\min && ||\underline{\boldsymbol{a}}||_p \\ &\text{subject to} && \underline{\tilde{\boldsymbol{\Phi}}}\,\underline{\boldsymbol{a}} = \underline{\boldsymbol{z}} \end{aligned} \tag{3.11}$$

For practical reasons, we choose $p = 0$ and minimize the ℓ_0 norm of $\underline{\boldsymbol{a}}$, i.e. find the minimum number of non-zero elements that satisfy the constraints. We use the ℓ_0 norm of an U-dimensional vector $\underline{\boldsymbol{a}}$

$$||\underline{\boldsymbol{a}}|| = \lim_{p \to 0} \sum_{r=1}^{R} |a_u|^p . \tag{3.12}$$

This ℓ_0 norm optimization problem, referred to as the sparse approximation problem [25], is hard to solve because of its highly nonlinear nature.

A technique to solve (3.11) is called the Orthogonal Matching Pursuit (*OMP*) algorithm, which is known as a "greedy" scheme [26], [27]. The *OMP* constructs iteratively an approximation to the solution.

An alternative approach is based on the relaxation of the equality constraints (3.11) to the inequality for a specified tolerance $\underline{\boldsymbol{\epsilon}}$, which achieves a solution with a greater number of zero elements in $\underline{\boldsymbol{a}}$. This approach explicitly recognizes that the vector $\underline{\boldsymbol{z}}$ is simply an estimate based on the speculator's analysis of the system's behavior and incorporates uncertainty. In this case, we formulate the optimization problem

$$\begin{aligned} &\min && ||\underline{\boldsymbol{a}}||_0 \\ &\text{subject to} && \underline{\boldsymbol{z}} - \underline{\boldsymbol{\epsilon}} \leq \underline{\tilde{\boldsymbol{\Phi}}}\,\underline{\boldsymbol{a}} \leq \underline{\boldsymbol{z}} + \underline{\boldsymbol{\epsilon}} \end{aligned} \tag{3.13}$$

where the vector $\underline{\boldsymbol{\epsilon}}$ specifies the tolerance.

Once $\underline{\boldsymbol{a}}$ is determined, the vectors specifying the U transactions $\underline{\boldsymbol{w}}_u = [m_u, q_u, a_u]^T$, $u = 1, \ldots, U$ are known. However, we only need the transactions with $a_u \neq 0$, and so select a subset with K elements, where $K \leq U$, that have $a_u \neq 0$. Since the K transactions satisfy the V specifications of the speculator, we may associate each transaction with the FTR for the node pair $\{m_u, n_u\}$ in the amount a_u to construct the portfolio. Thus, the set $\mathscr{F} = \{\Gamma_1, \ldots, \Gamma_K\}$, where $\{i_k, j_k, \gamma_k\}$ are given by

$$\Gamma_k = \{i_k = m_k, j_k = q_k, \gamma_k = a_k\},\ k = 1, \ldots, K\ . \tag{3.14}$$

Once we specify all Γ_k, we have the solution to the problem stated in (3.4)

In this chapter, we described the problem that the proposed approach is solving. We suggest a methodology for the speculator to specify a subset of congested lines that he wishes the FTR in the portfolio to include in their paths, and formulate the optimization problem of determining the FTR in the portfolio. In Chapter 4, we provide representative cases of the proposed method on three tests systems.

CHAPTER 4

APPLICATION STUDIES

We devote this chapter to illustrate the application of the *FTR* portfolio construction methodology of Chapter 3 to representative cases on three test systems. The test systems are a modified version of the *IEEE* 30-bus system, a modified version of the *IEEE* 118-bus system and the large-scale *PJM ISO* network. The small modified *IEEE* 30-bus system is an appropriate vehicle to explain the advantages of the proposed methodology so as to avoid the exhaustive evaluation of all possible *FTR* node pairs. For both the modified *IEEE* 118-bus system and the larger *PJM ISO* network, we provide a wide range of sensitivity studies to illustrate the well-behaved performance of the optimized portfolio construction algorithm. In these studies, we demonstrate the mechanics of the construction algorithm and discuss how we make use of the physical grid characteristics and the insights we gain from the solution. To make the discussion of the numerical results more manageable, we use a one month holding period for *FTR* contracts in the portfolio.

We devote one section to present the results for each test system, and in the last section we offer concluding remarks about the numerical results.

4.1 Description of Test Systems and Overview of Case Studies

We summarize the key characteristics of the three test systems and discuss a number of representative cases on the three systems.

The modified *IEEE* 30-bus system used has 41 lines, whose network topology may be found in [28]. The network topology of the system is depicted in Fig. 4.1. We use the coefficients of the *IEEE* reliability test system [29] and scale the load to have a peak value of 796 MW. We choose load and generation offer data to clear the *DAM*s for the *FTR* holding period in the

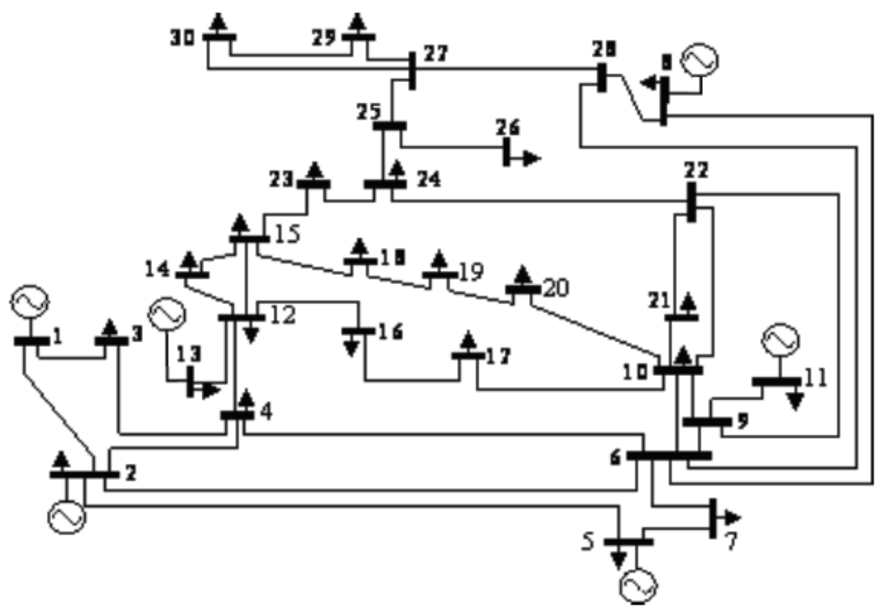

Figure 4.1: One line diagram of the *IEEE* 30-bus system

system to be as realistic as possible. The buyer bids are fixed demand bids which specify the *MW* quantity without any price information. Such bids indicate an unlimited willingness to pay for the electricity purchases. Also, we assume that the offer price of each seller remains unchanged during the period of one month and is considered to be a linear curve. The offer data are found in [30]. The modifications we made to the system may be found in D.2. We refer to the modified *IEEE* 30-bus system as system R.

The modified *IEEE* 118-bus system is based on the *ISO* New England (*ISONE*) network and has 186 lines, as shown Fig. C.1. We use a scaled version of the load for the *ISONE* of January 2010. The peak load of the scaled version is $2,922\,MW$ and we distribute it to the nodes. We treat the load as price insensitive and we clear the market with the use of generation offers curves, which change once in the period of one month. We use the offer curves of [30] from day 1 to day 16 and the offer curves in Table D.4 for the remaining period. As a result, the cheapest generation offered varies over the period of one month, causing certain lines to get congested. The real power line flow limits are set to be $170\,MW$ for all lines and the changes in topology are given in D.3. We refer to the modified *IEEE* 118-bus system as system S.

The *PJM ISO* system is truly large-scale, since it has 14,322 nodes and 19,787 lines. We use actual data of the transmission usage costs [2] and decide on the lines in the two subsets. The speculator participates in a monthly auction to purchase *FTR* with the holding period of September 1 to September 30 2010. We refer to the *PJM ISO* network as system T.

We provide a summary of the three tests systems' characteristics in Table 4.1.

Table 4.1: Key characteristics of the test systems

Test system	**description**	**number of nodes**	**number of branches**
R	*IEEE* 30-bus	30	41
S	*IEEE* 118-bus	118	186
T	*PJM ISO* network	14,322	19,787

For all cases in the three systems, the speculator uses historical data to choose lines in the two subsets and his level of participation, and buys *FTR* contracts that satisfy his requirements. For system R, we have two cases, one where we construct the *FTR* portfolio considering all possible node pairs and the other where we choose a subset of nodes to specify the *FTR* nodes pairs. We also change the input parameters of the second case to test the robustness of the methodology. The cases for system S are the construction of the optimized *FTR* portfolio, with some sensitivity cases, and the construction of the *FTR* portfolio by minimizing the *FTR MW* amount. For the large-scale system T, we find the optimized *FTR* portfolio and run some sensitivity cases to check the well-behaved performance of the methodology. We summarize the scope of the case studies in Table 4.2. We discuss the results of cases A-B in Section 4.2, those of cases C-D in 4.3 and that of case E in 4.4.

4.2 Test System R Studies

The speculator participates in a monthly auction and buys *FTR* of one month holding period. We use the *TUCDC*s in Fig. 4.2 along with the key causal factor of congestion to specify the two subsets and the level of participation on each line. For example, lines $(6, 7)$ and $(22, 24)$ get congested due to the changes in topology and the rest are mainly driven by the demand levels and

Table 4.2: Test cases

Case	Test system	description
case A	R	we choose all nodes to construct the portfolio
case B	R	we present the value of choosing a subset of nodes
		we modify the lines in the two subsets
case C	S	we present the value of the ℓ_0 minimization
		we modify the level of participation in the two subset by steps of 2.5% from $0-10\%$
case D	S	we specify the portfolio with minimum *FTR MW* euclidean norm amount
case E	T	construct the optimized *FTR* portfolio
		we modify the level of participation in the two subset by steps of 2.5% from $0-10\%$

are congested for a big fraction of the time. More specifically, the real power flow of line $(6,7)$ reaches its limiting value when line $(10,17)$ is outaged and that of line $(22,24)$ when line $(18,19)$ is outaged. Line $(1,2)$ is purely driven by demand levels and is not affected by the changes in topology. However, the transmission usage costs of lines $(6,8)$ and $(21,22)$ are affected by the changes in topology and reach higher values in the contingency cases of single line outage of $(10,17)$,$(27,29)$ and $(18,19)$ respectively. We may specify the speculator's requirements with the quadruplets given in Table 4.3.

Table 4.3: Input data for cases A-B

Input data	
ζ^1	$\{1,(1,2),10,\{\varnothing\}\}$
ζ^2	$\{1,(21,22),-10,\{\varnothing\}\}$
ζ^3	$\{0,(22,24),0,\{(18,19)\}\}$
ζ^4	$\{0,(6,8),0,\{\varnothing\}\}$
ζ^5	$\{0,(6,7),0,\{(10,17)\}\}$

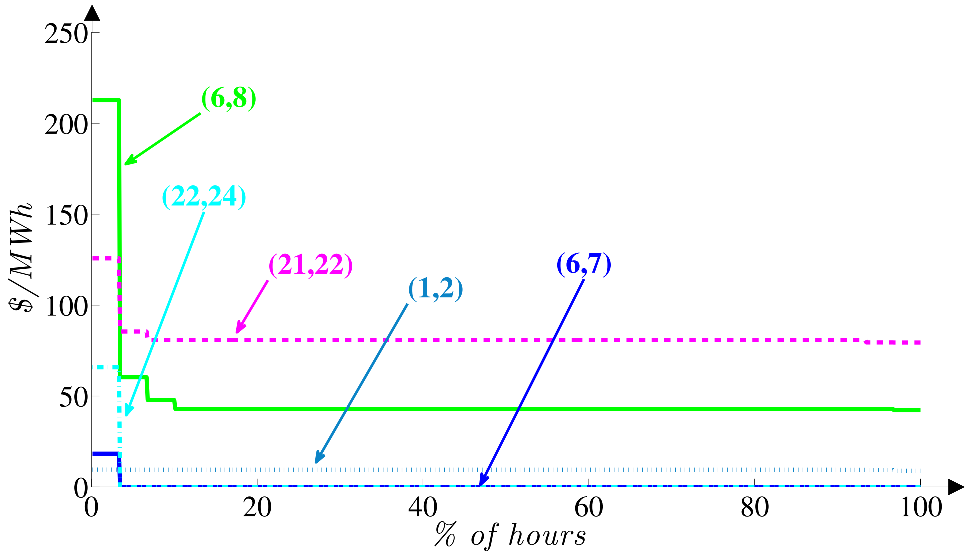

Figure 4.2: The annual $TUCDC$s for the congested lines of the test system R

Lines $(21, 22)$ and $(22, 24)$ get congested in the direction from 22 to 21 and 24 to 22 respectively. That is why we wish to induce a negative flow on line $(21, 22)$, so it has the same direction as congestion. The topologies considered are three; one is the base case with 30 nodes and 41 lines and the other two refer to a one-line outage that causes lines $(6, 7)$ and $(22, 24)$ to get congested respectively. We need to determine the transactions that induce the desired flows on the lines as specified by the speculator's requirements. In this small scale system, we may construct an FTR portfolio $\mathscr{F}_A$ by considering all possible node pairs to determine the minimum number of FTR in the portfolio. By solving the optimization problem we find the portfolio

$$\mathscr{F}_A = \big\{\{1, 2, 9.41\}, \{1, 9, 1.52\}, \{22, 21, 11.23\}\big\} .$$

For the computation of the revenues we make use of the outcomes of the DAMs for the holding period. Our interest is in the mechanics of the algorithm and we keep the data of the DAMs as simple as possible. The associated revenues for $\mathscr{F}_A$ are $\$692, 840$.

We now evaluate the optimized FTR portfolio for the same input data (Table 4.3), to show that the choice of a subset of nodes is meaningful by comparing the results of case A with those of case B. We choose a subset of nodes, as described in (3.6), and specify the set

$$\mathscr{H} = \{1, 2, 6, 7, 8, 21, 22, 24\} \ .$$

The possible node pairs for the transactions are given by the set

$$\begin{aligned}\mathscr{R} = \{&(1,2),(1,6),(1,7),(1,8),(1,21),(1,22),(1,24),(2,6),(2,7),(2,8),\\&(2,21),(2,22),(2,24),(6,7),(6,8),(6,21),(6,22),(6,24),(7,8),\\&(7,21),(7,22),(7,24),(8,21),(8,22),(8,24),(21,22),(21,24),(22,24)\} \ .\end{aligned}$$

After solving the optimization problem, we specify the minimum number of transactions and we associate them with *FTR*. The algorithm obtains the portfolio

$$\mathscr{F}_{B_0} = \big\{\{1, 2, 11.42\}, \{7, 21, 0.25\}, \{22, 2, 10.62\}\big\} \ .$$

The associated revenues for portfolios $\mathscr{F}_{B_0}$ are $\$662,520$, based on the outcomes of the *DAM*s for the *FTR* holding period.

For case A and B, we observe, that the number of *FTR* in $\mathscr{F}_{B_0}$ is the same as in $\mathscr{F}_A$. However, we notice that the *FTR MW* amounts that need to be purchased in the case of $\mathscr{F}_A$ are smaller in total by $0.13\,MW$ than those of $\mathscr{F}_{B_0}$. This is because an injection or withdrawal at node 9, which was not considered in the case of $\mathscr{F}_{B_0}$, changes the real power flow on the lines in the subsets to a great extent. However, the improvement of the portfolio outcomes is negligible when we include all possible node pairs, and the computational burden in doing so in a large scale system is big. We may conclude that the method we use is sufficient and balances the computational burden with achieving meaningful results. The revenues associated with portfolio $\mathscr{F}_A$ and $\mathscr{F}_{B_0}$ are $\$662,520$ and $\$692,840$ respectively, indicating a small difference. We discuss the cause for the difference in the revenues. We consider the transactions corresponding to the three *FTR* in the portfolio $\mathscr{F}_A$. The impact of these transactions is to set up a $-10\,MW$ flow on line $(21,22)$, i.e., a flow of $+10\,MW$ from node 22 to node 21, in the base case topology, as obtained from the *PTDF*s associated with those three transactions for line $(21,22)$. However, whenever a line outage occurs, the flow on line $(21,22)$ changes as given by the *OTDF*. Such line outage impacts are visible for the hours when such outages occur in terms of change in the values of the flows of line $(21, 22)$ and are shown in Fig. 4.3. Conceptually, any transactions

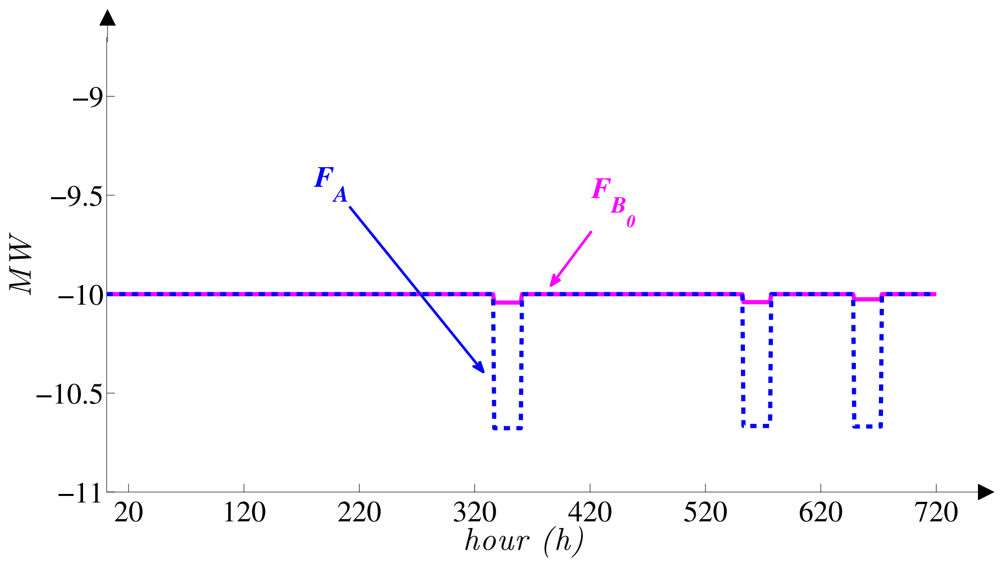

Figure 4.3: The plot of the hourly real power flow on line $(21, 22)$ of the test system R associated with the transactions corresponding to the FTR in $\mathscr{F}_A$ and $\mathscr{F}_{B_0}$

contribute to congestion. Absent transactions, the congested situation of line $(21, 22)$ ensures that the transmission usage cost contributes to the FTR revenues, as derived in (2.16). The same arguments may be expressed for the FTR in portfolio $\mathscr{F}_{B_0}$. In light of these insights, the different revenues are due to the different FTR in the portfolio, and therefore, to the different way that transactions with the same node pairs and amounts as FTR impact line $(21, 22)$ for every hour of the holding period.

In order to demonstrate the well behaved performance of the proposed scheme, we change the input parameters by adding additional lines in the two subsets. The input data of the optimized FTR portfolio are given in Table 4.4.

We construct the optimized FTR portfolio

$$\mathscr{F}_{B_1} = \big\{\{1, 2, 11.63\}, \{7, 2, 0.64\}, \{22, 2, 0.37\}, \{24, 2, 0.46\}, \{22, 21, 10.66\}\big\}\ .$$

The revenues of $\mathscr{F}_{B_1}$ are \$663, 410. Portfolio $\mathscr{F}_{B_1}$ contains two more FTR than $\mathscr{F}_{B_0}$. Two of the node pairs remain the same, but three new FTR are introduced in $\mathscr{F}_{B_1}$. We depict in Fig. 4.4 the real power flow on line $(6, 8)$

Table 4.4: Input data for sensitivity case of case B

Input data	
ζ^1	$\{1,(1,2),10,\{\varnothing\}\}$
ζ^2	$\{1,(21,22),-10,\{\varnothing\}\}$
ζ^3	$\{0,(22,24),0,\{(18,19)\}\}$
ζ^4	$\{0,(6,8),0,\{\varnothing\}\}$
ζ^5	$\{0,(6,7),0,\{(10,17)\}\}$
ζ^6	$\{0,(6,8),0,\{(10,17)\}\}$
ζ^7	$\{0,(6,8),0,\{(27,29)\}\}$

induced by transactions with the same node pairs and amounts as FTR in $\mathscr{F}_{B_0}$ and $\mathscr{F}_{B_1}$. We may see that transactions associated with $\mathscr{F}_{B_0}$ induce non-zero flows on line $(6,8)$, when line $(10,17)$ and $(27,29)$ are outaged.

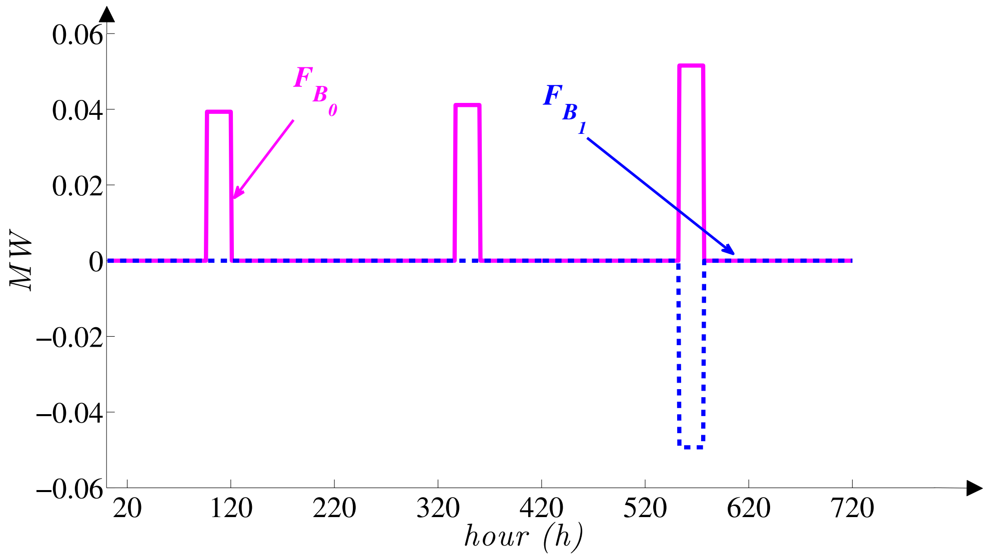

Figure 4.4: The plot of the hourly real power flow on line $(6,8)$ of the test system R associated with the transactions corresponding to the FTR in $\mathscr{F}_{B_0}$ and $\mathscr{F}_{B_1}$

In this small scale system, we demonstrated that the selection of a subset of nodes is appropriate for constructing the optimized FTR portfolio and that the revenues of an FTR portfolio are determined by the real power flows that transactions, with same node pairs and amounts as FTR, induce on the congested lines. The speculator, by his quadruplets, specifies his requirements, i.e. his level of participation on a set of congested lines, for a subperiod of the holding period. Two portfolios that satisfy the speculator's requirements have different revenues because the transactions associated with each portfolio affect the remaining lines for the entire period and the lines in his requirements for topologies different than that specified, in a different way. Moreover, we presented that the portfolio is well-behaved when the input parameters are modified.

4.3 Test System S Studies

The speculator participates in the January auction and buys FTR from January 1 to January 31. We use historical data of the transmission usage costs and determine the key causal factor of congestion to specify the speculator's requirements. The $TUCDC$s from historical data of three months, appropriately chosen to fit the characteristics of the holding period, are depicted in Fig. 4.5. We specify the input data in Table 4.5.

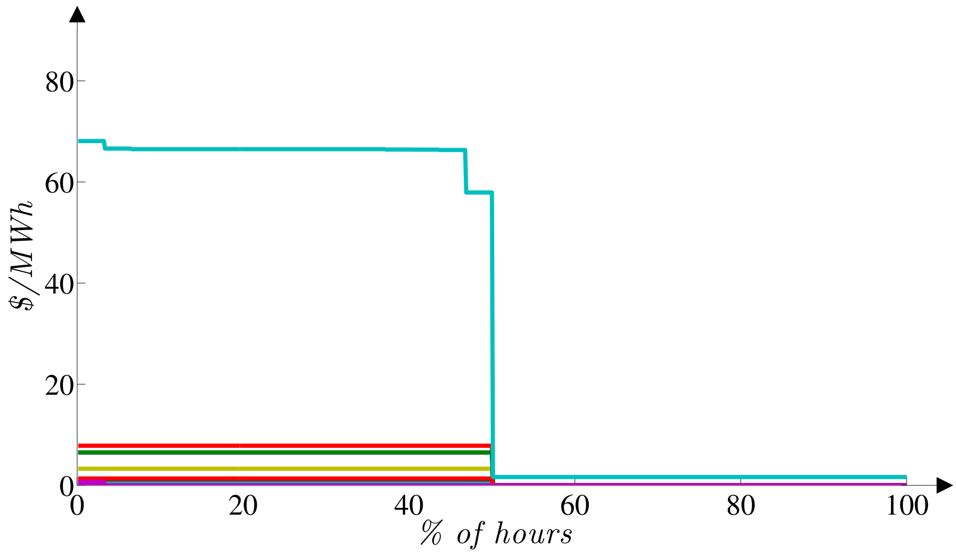

Figure 4.5: The three month $TUCDC$s for the congested lines of the test system S

As an example, we chose the quadruplet $\zeta^7 = \{1, (26, 30), 1, \{\varnothing\}\}$ because, as we can see from the $TUCDC$ shown in Fig. 4.6, the line is congested for a big fraction of time in the past. Line $(26, 30)$ gets congested due to the fuel prices that affect the offer curves of generators. Based on historical data, the generator in node 26 offers cheap energy. So, since the speculator assumes

Table 4.5: Input data for case C and D

Input data	
ζ^1	$\{0,(8,9),0,\{\varnothing\}\}$
ζ^2	$\{0,(64,65),0,\{\varnothing\}\}$
ζ^3	$\{1,(89,92),1,\{\varnothing\}\}$
ζ^4	$\{1,(38,65),-1,\{\varnothing\}\}$
ζ^5	$\{1,(68,116),1,\{\varnothing\}\}$
ζ^6	$\{1,(9,10),-1,\{\varnothing\}\}$
ζ^7	$\{1,(26,30),1,\{\varnothing\}\}$
ζ^8	$\{1,(8,5),1,\{\varnothing\}\}$
ζ^9	$\{0,(38,37),0,\{\varnothing\}\}$
ζ^{10}	$\{0,(30,17),0,\{\varnothing\}\}$
ζ^{11}	$\{0,(65,68),0,\{\varnothing\}\}$

that the future is a continuation of the past, he wishes to specify FTR such that transactions with the same node pairs and amounts induce $1\,MW$ of real power flow on line $(26,30)$. The $TUCDC$ of line $(68,116)$ is also depicted in Fig. 4.6. Line $(68,116)$ is driven by the demand levels, which make the IGO utilize more the transmission network, causing the flow on some lines to reach their maximum limit. Similar arguments may be used for the rest of the quadruplets.

We next choose the subset of nodes that are terminal nodes of the lines in the two subsets. So we choose the set of nodes

$$\mathscr{H} = \{5,8,9,10,17,26,30,37,38,64,65,68,89,92,116\}\ . \tag{4.1}$$

We construct the possible node pairs $\mathscr{R}$ as discussed in (3.7) and solve the minimization problem with objective the ℓ_0 of the vector of amounts in MW subject to the speculator's requirements given by the quadruplets. The solution to this optimization problem is

$$\mathscr{F}_{C_0} = \big\{\{10,9,1.00\},\{26,38,1.50\},\{65,37,0.73\},\{64,38,0.16\},\\ \{65,38,0.36\},\{65,92,0.14\},\{68,92,3.22\},\{89,116,1.02\}\big\}\ .$$

The minimum number of FTR pairs is 8 in order to meet the speculator's requirements and the total FTR amount is $8.13\,MW$. The associ-

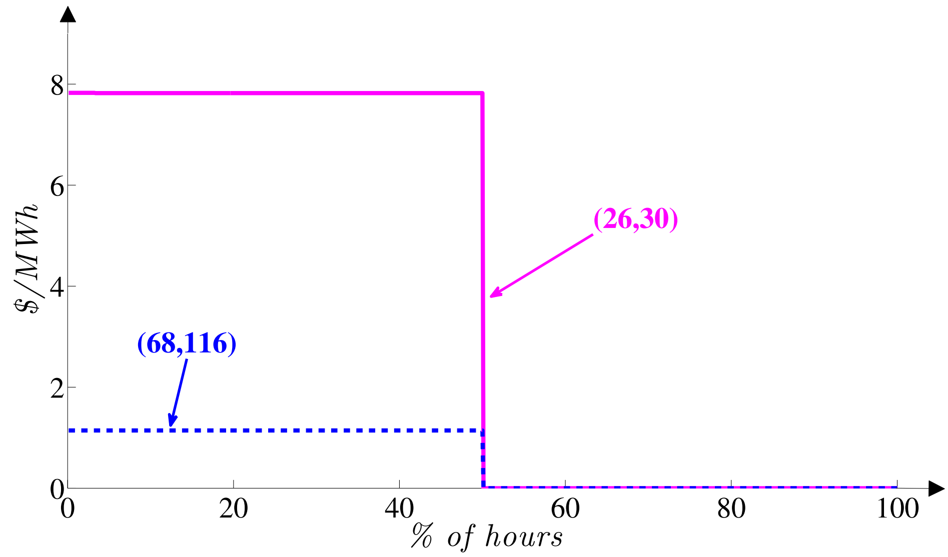

Figure 4.6: The three month $TUCDC$s for lines $(26, 30)$ and $(68, 116)$ of the test system S

ated revenues are $\$7,467$. We plot the LMP differences for the node pairs $\{65, 38\}, \{68, 92\}$ and $\{26, 38\}$ for every hour of January in Fig. 4.7. We notice that the LMP differences are positive for every hour of the holding period. This is due to the fact that the paths of each node pair include the congested lines in the congested direction.

We choose to relax the constraints in the optimization problem. We modify the participation level of the speculator on each line as given in Table 4.5. The optimization problem was

$$\begin{aligned} &\min && ||\underline{\boldsymbol{a}}|| \\ &\text{subject to} && \underline{\tilde{\boldsymbol{\Phi}}}\,\underline{\boldsymbol{a}} = \underline{\boldsymbol{z}}\ . \end{aligned} \tag{4.2}$$

We modify (4.2) by considering a new set of constraints

$$\underline{\boldsymbol{z}}\,(1-\epsilon) \leq \underline{\tilde{\boldsymbol{\Phi}}}\,\underline{\boldsymbol{a}} \leq \underline{\boldsymbol{z}}\,(1+\epsilon)\ . \tag{4.3}$$

We modify ϵ uniformly, in steps of 2.5% from $[2.5\%, 10\%]$, and demonstrate the results in Table. 4.6.

As we increase the value of ϵ, we augment the feasibility region. As a result, the outcomes of the proposed method include FTR portfolios with fewer node pairs and less total MW amount than the FTR portfolio for $\epsilon = 0\%$. The

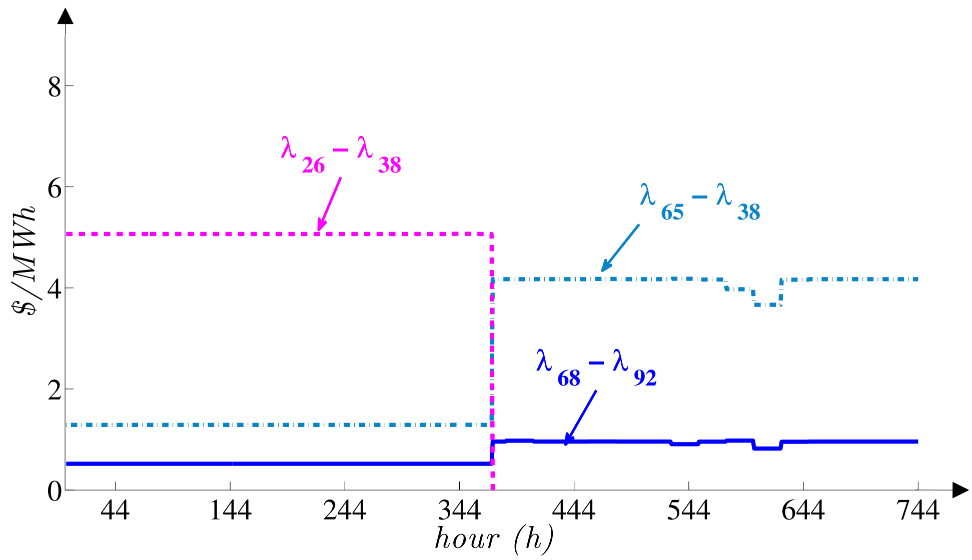

Figure 4.7: The plot of the hourly LMP differences at 3 node pairs in the test system S during a 31 day month

Table 4.6: Results of the sensitivity cases of system S

Sensitivity cases ϵ	Symbol	***FTR*** portfolio elements	number of nodes pairs	total ***FTR*** MW amount	revenues (\$)
0%	$\mathscr{F}_{C_0}$	$\{\{10,9,1.00\}$, $\{26,38,1.50\}$, $\{65,37,0.73\}$, $\{64,38,0.16\}$, $\{65,38,0.36\}$, $\{65,92,0.14\}$, $\{68,92,3.22\}$, $\{89,116,1.00\}\}$	8	8.13	7467
2.5%	$\mathscr{F}_{C_1}$	$\{\{10,9,0.97\}$, $\{26,38,1.48\}$, $\{65,37,0.69\}$, $\{64,38,0.18\}$, $\{65,38,0.34\}$, $\{65,92,0.15\}$, $\{68,92,3.21\}$, $\{89,116,0.98\}\}$	8	8.10	6837
5%	$\mathscr{F}_{C_2}$	$\{\{10,9,0.95\}$, $\{26,38,1.47\}$, $\{65,37,0.68\}$, $\{64,38,0.17\}$, $\{65,38,0.42\}$, $\{65,92,0.18\}$, $\{68,92,3.19\}$, $\{89,116,1.00\}\}$	8	8.06	7116
7.5%	$\mathscr{F}_{C_3}$	$\{\{10,9,0.96\}$, $\{26,38,1.44\}$, $\{65,37,0.63\}$, $\{64,38,0.12\}$, $\{65,38,0.45\}$, $\{68,92,3.18\}$, $\{89,116,1.10\}\}$	7	7.88	7785
10%	$\mathscr{F}_{C_4}$	$\{\{10,9,0.89\}$, $\{26,38,1.43\}$, $\{65,37,0.65\}$, $\{64,38,0.14\}$, $\{65,38,0.40\}$, $\{68,92,3.09\}$, $\{89,116,0.96\}\}$	7	7.56	7785

minimization of the ℓ_0 norm has a close relationship with that of the ℓ_1 norm. Therefore, when we augment the feasibility region, the ℓ_1 norm of vector $\underline{\boldsymbol{a}}$ is also decreased, as may be seen in Table 4.6 and Fig. 4.8. We notice that the proposed methodology is well-behaved, since $\mathscr{F}_{C_1}$ and $\mathscr{F}_{C_2}$ have the same node pairs but different MW amounts and $\mathscr{F}_{C_3}$ and $\mathscr{F}_{C_4}$ have one less FTR. The FTR revenues for each portfolio depend on the flows that transactions, with same node pairs and amounts, induce on the congested lines. For example, we depict in Fig. 4.9 the flows on line $(38, 65)$ induced by

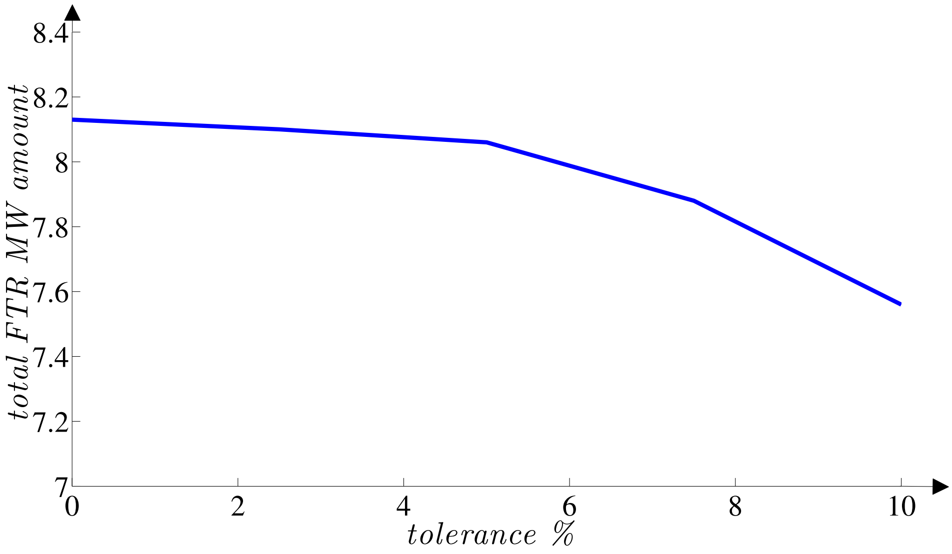

Figure 4.8: The variation of the sum of the FTR amounts as a function of the uniform tolerance ϵ in the speculator's participation level for system S

the transactions associated with each portfolio. From Fig. 4.9, we see that

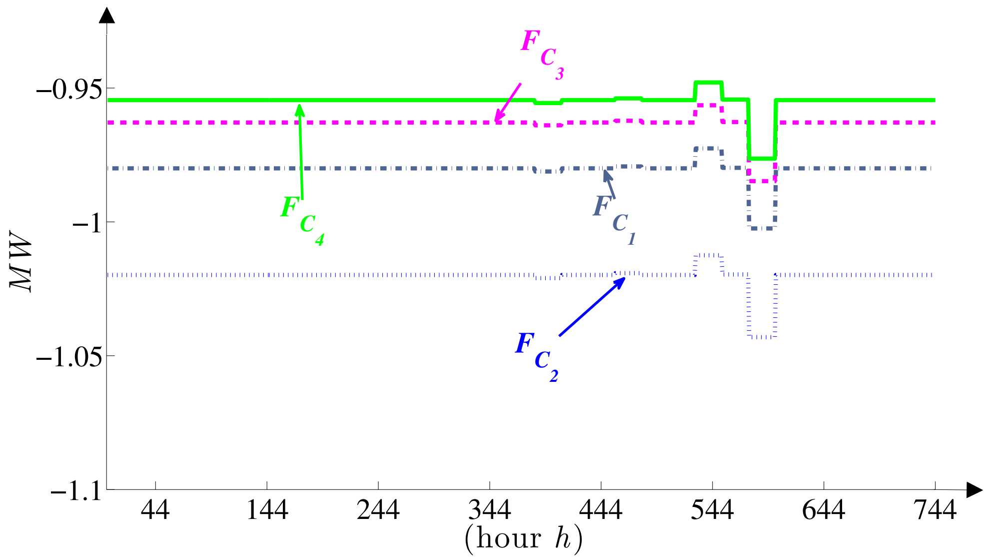

Figure 4.9: The plot of the hourly real power flow on line $(38, 65)$ of the test system S associated with the transactions corresponding to the FTR in $\mathscr{F}_{C_1}, \mathscr{F}_{C_2}, \mathscr{F}_{C_3}$ and $\mathscr{F}_{C_4}$

as we increase the value of ϵ the flow on line $(38, 65)$ moves away from the original value specified by the speculator at $1\,MW$.

We use the input, given in Table 4.5, and determine the FTR portfolio with the minimum MW norm; i.e., we modify the objective function and instead of the ℓ_0 minimization, we minimize the euclidean norm ℓ_2. The FTR portfolio includes 136 FTR and the total FTR amount is 7.69 MW. The total FTR amount of $\mathscr{F}_{C_0}$ is greater by 0.44 MW. The FTR revenues for $\mathscr{F}_D$ are $\$7,458$. We demonstrate the hourly revenues of two FTR in the portfolio $\{10, 5, 0.07\}$ and $\{100, 8, 0.03\}$ in Fig. 4.10. We notice that the contribution in the total revenues of each FTR in the portfolio $\mathscr{F}_D$ is very small, but since their number is large, the total revenues are large.

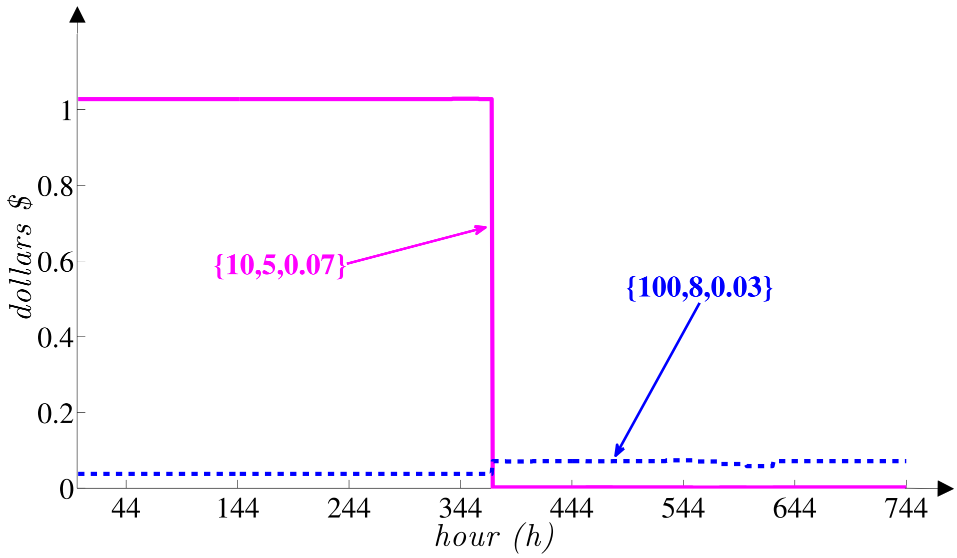

Figure 4.10: The plot of the hourly revenues for FTR $\{10, 5, 0.07\}$ and $\{100, 8, 0.03\}$ in system S for the holding period

The difference in the revenues of $\mathscr{F}_{C_0}$ and $\mathscr{F}_D$ is due to the different paths of the FTR in each portfolio. As described in Section 4.2 the transactions with the same node pairs and amounts as the FTR in each portfolio affect the lines in the two subsets in different ways for topologies other than those specified in the quadruplets. In order to understand the difference in the revenues, we also examine the flows on lines in the do-not-care congestion participation subset. We focus on those that get congested, since they impact the FTR revenues. For this case, this happens only for line $(100, 103)$. As shown in Fig. 4.11a, the line $(100, 103)$ is congested for some hours with transmission usage cost less than $1\$/MWh$. The real power flow that transactions associated with each portfolio induce on the line are given in Fig. 4.11b. Congestion in line $(100, 103)$ is in the direction from 103 to

100, so when transactions associated with $\mathscr{F}_D$ have positive flows on the line as seen in Fig. 4.11b the revenues of $\mathscr{F}_D$ are reduced; in the case of $\mathscr{F}_{C_0}$ we have the opposite effect.

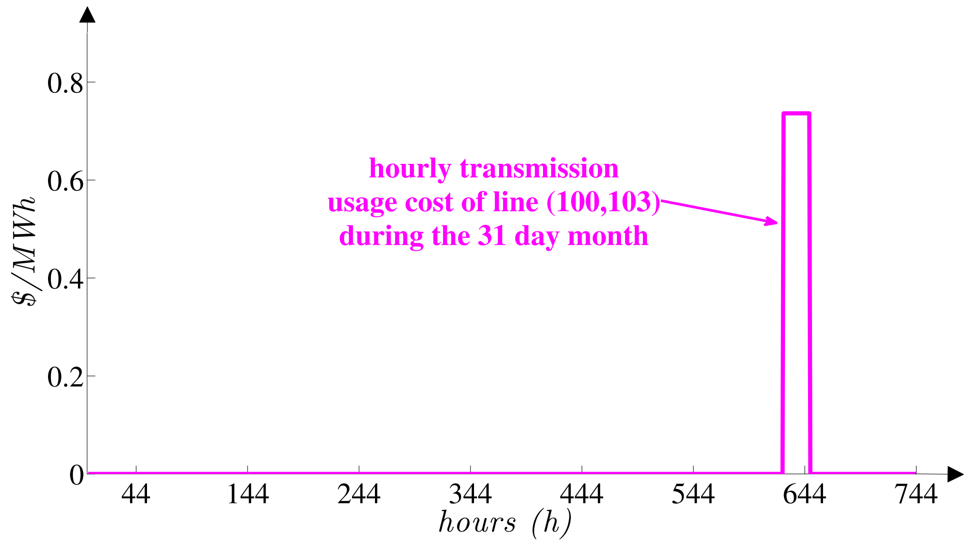

(a)

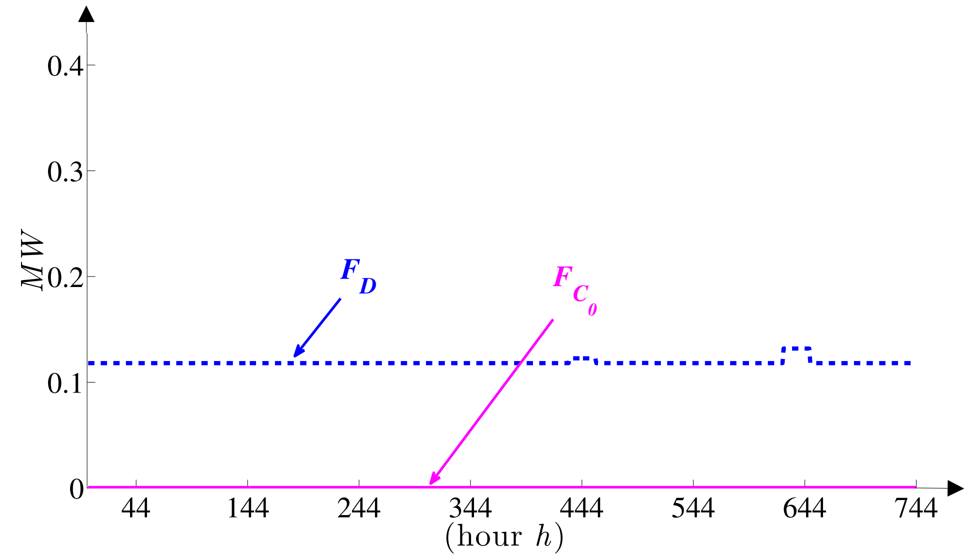

(b)

Figure 4.11: (a) Hourly transmission usage cost of line $(100, 103)$ and (b) the real power flow on the line $(100, 103)$ of the test system S associated with the transactions corresponding to the FTR in $\mathscr{F}_{C_0}$ and $\mathscr{F}_D$

4.4 Test System T Studies

The speculator participates in the September monthly auction and wishes to purchase *FTR* that increase his returns. He makes use of historical data [2], as described in Section 3.2, to specify his requirements. The speculator determines two price and time fraction thresholds to specify the quadruplets. We present in Fig. 4.12a and 4.12b, the *TUCDC*s of two lines: Doubs and Albright-Sno. Since the two lines were congested in the past and their transmission usage costs have high values, i.e., they exceed the specified thresholds, they are included in the quadruplets. Similar analysis for the remaining lines of the *PJM ISO* system is made and the quadruplets are specified. Therefore the inputs to the proposed scheme are given in Table 4.7. We next choose the subset of nodes that are terminal nodes of the lines in

Table 4.7: Input data of the proposed scheme

Line	MW **amount**
Ruth	0
Millvill-Old	100
Millvill-Sle	100
Chuckatk	0
Mardela-Vie	100
Albright-Sno	100
Nipetown-Rei	100
Doubs	100
OX4	0
Halfway-Mar	0
England-Mdt	0
Kingwood-Pru	0

the two subsets and solve the minimization problem with objective the ℓ_0 of the vector of amounts in MW subject to the speculator's requirements given in Table 4.7. The solution to this optimization problem is

$$\mathscr{F}_{E_0} = \big\{\{2761, 2276, 56\}, \{2806, 2276, 114\}, \{2664, 2416, 106\}, \{2512, 2682, 441\}, \{2512, 2710, 434\}, \{2512, 2761, 3\}, \{2664, 2710, 147\}, \{2761, 2727, 12\}\big\} .$$

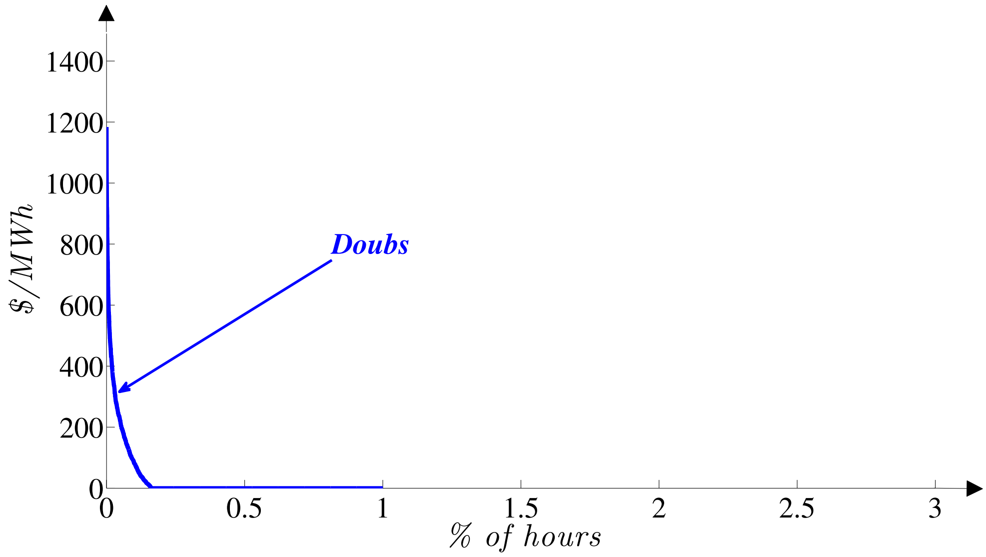

(a)

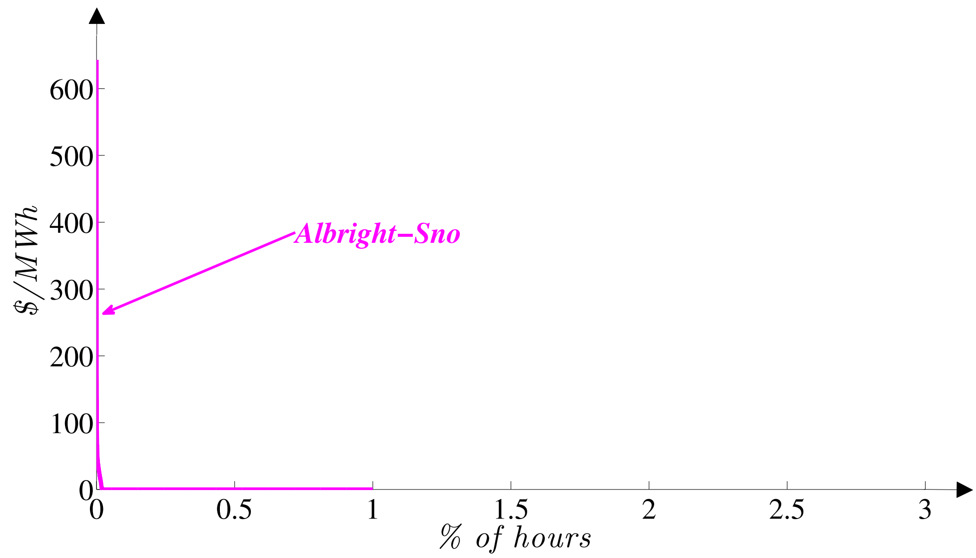

(b)

Figure 4.12: $TUCDC$s for 2 lines in the test system T based on historical data of a nine month period

The minimum number of FTR pairs is 8 in order to meet the speculator's requirements, and the total MW FTR amount is 1313. We present in Table D.5, the names associated with each node number. We depict in Fig. 4.13 the hourly LMP differences of node pair $\{2761, 2276\}$ for September 2010, as well as the mean value. We may see that the LMP difference is positive for the biggest fraction of the month. However, the negative value indicates that

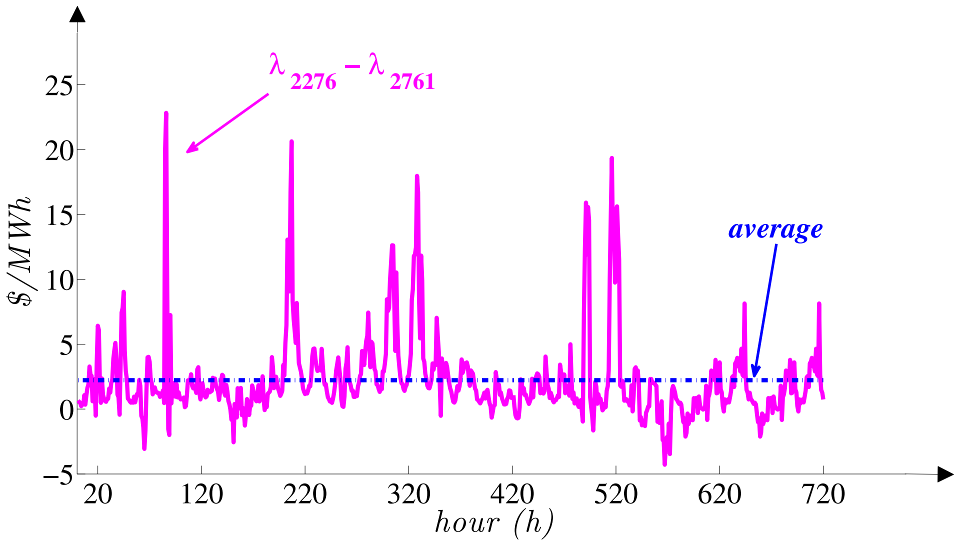

Figure 4.13: The plot of the hourly *LMP* differences between nodes 2761 and 2276 during September 2010 in system *T*

a transaction from 2761 to 2276 induces flows in the opposite direction of congestion in some lines. The mean value of the *LMP* difference is positive; therefore, the *FTR* revenues of {2761,2276,0.56} are positive for the holding period of September 2010.

According to the same notion as in Section 4.3, we relax the imposed constraints by several values of ϵ. The results of the optimized *FTR* portfolio are shown in Table 4.8.

Table 4.8: Results of the sensitivity cases of system *T*

Sensitivity cases ϵ	Symbol	***FTR*** portfolio elements	number of nodes pairs	total ***FTR*** MW amount
0%	$\mathscr{F}_{E_0}$	$\{\{2761, 2276, 56\}$, $\{2806, 2276, 114\}$, $\{2664, 2416, 106\}$, $\{2512, 2682, 444\}$, $\{2512, 2710, 434\}$, $\{2512, 2761, 3\}$, $\{2664, 2710, 147\}$, $\{2761, 2727, 12\}\}$	8	1312
2.5%	$\mathscr{F}_{E_1}$	$\{\{2761, 2276, 53\}$, $\{2806, 2276, 113\}$, $\{2664, 2416, 105\}$, $\{2512, 2682, 439\}$, $\{2512, 2710, 432\}$, $\{2512, 2761, 2\}$, $\{2664, 2710, 145\}$, $\{2761, 2727, 11\}\}$	8	1300
5%	$\mathscr{F}_{E_2}$	$\{\{2761, 2276, 52\}$, $\{2806, 2276, 110\}$, $\{2664, 2416, 104\}$, $\{2512, 2682, 438\}$, $\{2512, 2710, 430\}$, $\{2512, 2761, 1\}$, $\{2664, 2710, 144\}$, $\{2761, 2727, 10\}\}$	8	1289
7.5%	$\mathscr{F}_{E_3}$	$\{\{2761, 2276, 51\}$, $\{2806, 2276, 107\}$, $\{2664, 2416, 102\}$, $\{2512, 2682, 436\}$, $\{2512, 2710, 428\}$, $\{2664, 2710, 143\}$, $\{2761, 2727, 8\}\}$	7	1275
10%	$\mathscr{F}_{E_4}$	$\{\{2761, 2276, 50\}$, $\{2806, 2276, 103\}$, $\{2664, 2416, 100\}$, $\{2512, 2682, 437\}$, $\{2512, 2710, 425\}$, $\{2664, 2710, 143\}$, $\{2761, 2727, 10\}\}$	7	1268

The conclusions are similar to those derived in Section 4.3. It is interesting that the proposed methodology behaves well in such a large-scale system. We notice that the outcomes of the proposed method include *FTR* portfolios with fewer node pairs and less total *MW* amount than the *FTR* portfolio as we increase the value of $\epsilon = 0$, as depicted in Fig. 4.14. We notice that

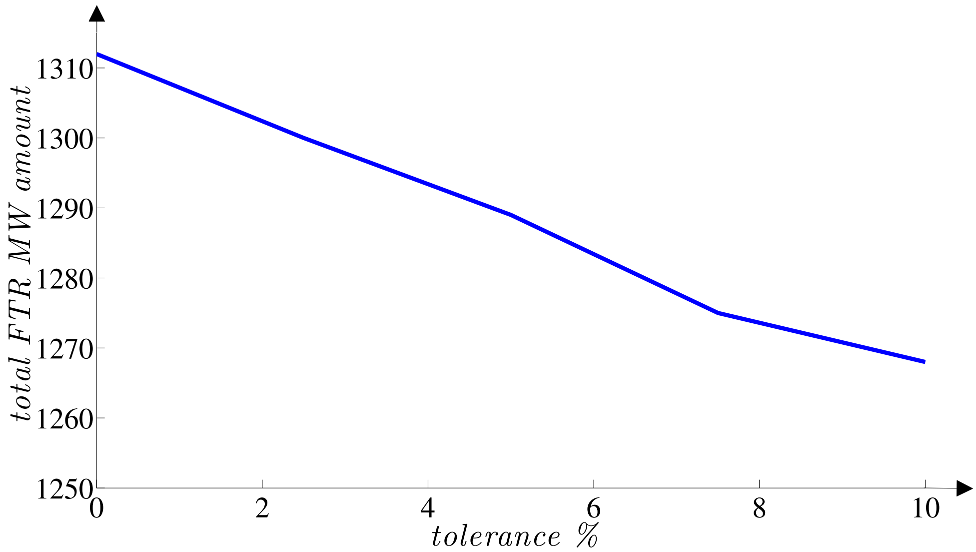

Figure 4.14: The variation of the sum of the *FTR* amounts as a function of the uniform tolerance ϵ in the speculator's participation level for system *T*

the proposed methodology is robust, since $\mathscr{F}_{E_1}$ and $\mathscr{F}_{E_2}$ have the same node pairs but different *MW* amounts and $\mathscr{F}_{E_3}$ and $\mathscr{F}_{E_4}$ have one less *FTR*.

4.5 Concluding Remarks

The studies described in this chapter quantify the range of benefits by using the proposed portfolio construction approach. We used the modified *IEEE* 30-bus system to focus on the key results and the essential insights obtained from the case studies, since such a small-scale system aids in the understanding of the proposed method. The modified *IEEE* 118-bus system is used to demonstrate the effectiveness of the proposed method for large-scale systems. More precisely, we demonstrate not only the efficiency of our approach, in terms of computational burden, but also the robustness of the results, through a thorough sensitivity analysis. The implementation of the proposed methodology in the large-scale system of *PJM ISO* indicates that it may be implemented in real systems.

From an extensive number of cases, a representative number of which are discussed in this chapter, we gain insight into the determination of the *FTR* revenues. The results made concrete that the revenues depend on the level of participation that the *FTR* in the portfolio have in (1) the specified congestion participation lines in the specified topology, (2) the specified congestion participation and zero congestion participation lines in different topologies than those specified in the speculator's requirements, and (3) the do-not-care congestion participation lines.

In addition, we showed that the selection of a subset of nodes in the determination of *FTR* possible node pairs is meaningful and reduces the computational burden in large-scale systems to a great extent. Moreover, the proposed methodology is robust, since the sensitivity cases show that the node pairs of the reference portfolio, for $\epsilon = 0\%$, and the sensitivity portfolios are the same for small values of ϵ, but the *FTR MW* amounts are smaller. For larger values of ϵ, the number of *FTR* in the portfolio is less than that of the reference case. These effects are due to the fact that we augment the feasibility region of the solution by increasing the value of ϵ.

CHAPTER 5

CONCLUSIONS

We present in this thesis the construction of an optimized *FTR* portfolio for a speculator. Since speculators are important players in the *FTR* auction, the construction of an optimized *FTR* portfolio for speculators is important. The uncertainty of the outcomes of the *FTR* auctions and *DAM*s of the holding period results in uncertainty of the speculator's returns, making his problem hard to manage. We solve a simplified problem, in which all *FTR* in the portfolio are contracts of the same holding period. In addition, we do not consider any previous *FTR* holding the speculator might have. When we focus on the *LMP* difference of the node pairs to select *FTR*, the number of all possible combinations is too demanding a task. Thus, we recast the problem by using the insights we gained from the analysis of the *DAM* clearing mechanism in Section 2.2, and base the *FTR* selection on the transmission usage costs of the congested lines.

More specifically, we select *FTR* that have congested lines in their paths from the source to the sink nodes. However, not all congested lines may be on the *FTR* paths for every hour of the holding period. Thus, we select a subset of lines by using historical data and topological characteristics of the underlying network. In particular, we use the *TUCDC*s of each line and specify two price and time fraction thresholds to reduce the number of lines we wish to include in the *FTR* paths. In addition, we determine the key causal factor of congestion, such as demand levels, fuel price trends and topology changes, to find which lines are likely to get congested in the holding period. On this basis the two subsets of lines, "specified congestion participation" and "zero congestion participation," are identified, as described in Section 3.2. Conceptually, we specify *FTR* such that transactions with the same node pairs and amounts as *FTR* induce real power flow, according to the desired level of participation, on the lines in the two subsets. In order to specify the transaction node pairs we choose a subset of nodes, taking into consideration the physical characteristics of the system. We construct the *FTR* portfolio with minimum number of node pairs; i.e., we specify the minimum number of transactions that cause the desired level of congestion participation on lines in the two subsets. We present a number of representative cases to show the implementation of the proposed method in different scale systems and check its robustness.

There are a number of natural extensions of the work presented here. The same approach may be extended to applications for hedging purposes. In such cases, the physical flows of the traders must be taken into account. However, the common characteristics of the hedging and speculative problems can be exploited in designing a practical solution approach. In particular, the modifications needed to recast the problem to the identification of a subset of congested lines requires further study.

Moreover, the portfolio definition may be extended to include additional aspects of the *FTR* problem such as the impacts of existing holdings and the ability to purchase and sell multiple *FTR* products, including different holding periods and *FTR* types. In such cases, the complexity of the problem is increased, but the insights we gained from the analysis of the *DAM* clearing mechanism still hold and can be exploited to construct practical solutions.

Another extension is the investigation of the formulation of bidding strategies in the *FTR* auction that are explicitly based on the speculator's requirements, such as the specification of the subset of congested lines chosen and the associated levels of participation. This problem can be addressed by developing mathematical insights from the formulation of the auction clearing mechanism. Furthermore, the development of metrics to quantify the risks associated with holding *FTR*, such as value at risk and conditional value at risk, is a good topic for further study.

APPENDIX A

MATHEMATICAL FORMULATION OF THE *FTR* AUCTION

We use the network description in Section 2.1 to formulate the primary *FTR* auction for *FTR* contracts. In the *FTR* auction model, the transmission constraints for the base case and the single-line outage contingency cases are expressed in terms of the *PTDF*s ($\phi_\ell^{\{i,j\}}$) and *OTDF*s ($\nu_{\ell\ell'}^{\{i,j\}}$). A buyer's b k bid for *FTR* is represented by $\left\{\overline{\Gamma}_k^{(b)}, \overline{c}_k^{(b)}\right\}$, where $\overline{\Gamma}_k^{(b)} = \{i_k^{(b)}, j_k^{(b)}, \overline{\gamma}_k^{(b)}\}$, $k = 1, \ldots K^{(b)}$. The clearing of the *FTR* auction is determined by solving an optimization problem, where the desired *FTR* are represented by actual transactions. The objective of the optimization problem is to maximize the bid-based value of *FTR*, with all the physical constraints not violated. We formulate the *FTR* auction clearing mechanism as follows:

$$
\begin{aligned}
\max \quad & \sum_{b=1}^{\mathbb{B}} \sum_{k=1}^{K^{(b)}} \overline{c}_k^{(b)} \gamma_k^{(b)} \\
\text{subject to} \quad & \sum_{b=1}^{\mathbb{B}} \sum_{k=1}^{K^{(b)}} \phi_\ell^{\{i_k^{(b)}, j_k^{(b)}\}} \gamma_k^{(b)} \le \zeta_\ell f_\ell^M, \ \ell = \ell_1, \ldots, \ell_L && \longleftrightarrow \beta_\ell^M \\
& \sum_{b=1}^{\mathbb{B}} \sum_{k=1}^{K^{(b)}} \phi_\ell^{\{i_k^{(b)}, j_k^{(b)}\}} \gamma_k^{(b)} \ge -\zeta_\ell f_\ell^m, \ \ell = \ell_1, \ldots, \ell_L && \longleftrightarrow \beta_\ell^m \\
& \sum_{b=1}^{\mathbb{B}} \sum_{k=1}^{K^{(b)}} \nu_{\ell\ell'}^{\{i_k^{(b)}, j_k^{(b)}\}} \gamma_k^{(b)} \le \zeta_\ell f_\ell^M, \ \ell, \ell' = \ell_1, \ldots, \ell_L && : \ell' \ne \ell \\
& \sum_{b=1}^{\mathbb{B}} \sum_{k=1}^{K^{(b)}} \nu_{\ell\ell'}^{\{i_k^{(b)}, j_k^{(b)}\}} \gamma_k^{(b)} \ge -\zeta_\ell f_\ell^m, \ \ell, \ell' = \ell_1, \ldots, \ell_L && : \ell' \ne \ell
\end{aligned}
\tag{A.1}
$$

where ζ_ℓ is the available system capability for each *FTR* auction.

APPENDIX B

PROOF OF THE LINE FLOW RESTRICTION LEMMA

We consider a power system consisting of the set of $(N+1)$ nodes $\mathscr{N} = \{0, 1, \ldots, N\}$, with the slack bus at node 0, and the set of L lines $\mathscr{L}$. We assume that the power system is lossless and that the DC power flow conditions hold. We use the notation $\mathscr{G}(\mathscr{N}, \mathscr{L})$ to denote the undirected graph associated with the network.

Proposition 1. In the connected network $\{\mathscr{N}, \mathscr{L}\}$, the minimum number of lines L is N.

Proof. We prove this proposition by making use of the graph $\mathscr{G}(\mathscr{N}, \mathscr{L})$. A network is connected if and only if there exists a path from every node to any other node of the network $\{\mathscr{N}, \mathscr{L}\}$ [31, p.3]. A connected network with a minimum number of lines is called a tree. Any tree of the network with the set of nodes $\mathscr{N}$ contains N lines [31, pp.115-116]. The minimum number of lines in a connected network $\{\mathscr{N}, \mathscr{L}\}$ is N. This minimality characterization of a tree implies that the connected network is characterized by $|\mathscr{L}| = L \geq N$. □

Proposition 2. In a connected network $\{\mathscr{N}, \mathscr{L}\}$, we can specify the flows on any set of K lines as long as a loop does not exist in the set of lines.

Proof. We prove the proposition by contradiction. We choose a set of lines, some of which form a loop, and then show that we may not specify the flows on all the K lines. We denote the subset $\mathscr{K} \subset \mathscr{L}$ of the K selected lines by $\mathscr{K} = \{\ell_1 = (i_1, j_1), \ell_2 = (i_2, j_2), \ldots, \ell_K = (i_K, j_K)\}$. Since a loop exists, we denote by $\mathscr{K}' \subset \mathscr{K}$, $\mathscr{K}' = \{\ell'_1 = (i'_1, j'_1), \ell'_2 = (i'_2, j'_2), \ldots, \ell'_{K'} = (i'_{K'}, j'_{K'})\}$, the subset of lines that form the loop. The elements of $\mathscr{K}'$ are ordered so that $i'_k = j'_{k-1},\ k = 2, \ldots, K'$ and $i'_1 = j'_{K'}$. The active power flow P_ℓ on line $\ell = (i, j)$ satisfies

$$P_\ell = (\theta_j - \theta_i)\, b_{ij}\ , \tag{B.1}$$

where θ_i (θ_j) is the voltage phase angle at node i (j) and b_{ij} is the susceptance of the line ℓ. The set of active power flow equations for the lines in $\mathscr{K}'$ forms the system of equations

$$\underline{\hat{\boldsymbol{P}}}_\ell = \underline{\hat{\boldsymbol{\Sigma}}}\,\underline{\hat{\boldsymbol{\theta}}}\ , \tag{B.2}$$

where

$$\underline{\hat{\boldsymbol{P}}}_\ell = \begin{bmatrix} P_{\ell'_1} \\ P_{\ell'_2} \\ \vdots \\ P_{\ell'_{K'}} \end{bmatrix} ,\ \underline{\hat{\boldsymbol{\Sigma}}} = \begin{bmatrix} \underline{\boldsymbol{\sigma}}_1^T \\ \underline{\boldsymbol{\sigma}}_2^T \\ \vdots \\ \underline{\boldsymbol{\sigma}}_{K'}^T \end{bmatrix} = \begin{bmatrix} b_{j'_{K'}j'_1} & 0 & \dots & 0 & -b_{j'_{K'}j'_1} \\ -b_{j'_1j'_2} & b_{j'_1j'_2} & \dots & 0 & 0 \\ \vdots & \vdots & \ddots & \vdots & \vdots \\ 0 & 0 & \dots & -b_{j'_{K'-1}j'_{K'}} & b_{j'_{K'-1}j'_{K'}} \end{bmatrix}$$

$$\text{and } \underline{\hat{\boldsymbol{\theta}}} = \begin{bmatrix} \theta_{j'_1} \\ \theta_{j'_2} \\ \vdots \\ \theta_{j'_{K'}} \end{bmatrix} .$$

The rank of the matrix $\underline{\hat{\boldsymbol{\Sigma}}}$ is less than K' since any row may be expressed as a linear combination of all the other rows of the matrix. This fact stems from the relationship

$$\underline{\boldsymbol{\sigma}}_k^T = \begin{cases} -\sum\limits_{\substack{\mu=1 \\ \mu\neq k}}^{K'} \dfrac{b_{j'_{K'}j'_1}}{b_{j'_{\mu-1}j'_\mu}}\,\underline{\boldsymbol{\sigma}}_\mu^T & k=1 \\ \\ -\sum\limits_{\substack{\mu=1 \\ \mu\neq k}}^{K'} \dfrac{b_{j'_{k-1}j'_k}}{b_{j'_{\mu-1}j'_\mu}}\,\underline{\boldsymbol{\sigma}}_\mu^T & k=2,\dots,K'\ . \end{cases} \tag{B.3}$$

Another way of writing (B.3) is

$$\sum_{k=1}^{K'} a_k\,\underline{\boldsymbol{\sigma}}_k^T = \underline{\boldsymbol{0}}^T \text{ or } \underline{\boldsymbol{a}}^T\,\underline{\hat{\boldsymbol{\Sigma}}} = \underline{\boldsymbol{0}}^T\ , \tag{B.4}$$

where a_k are determined by (B.3), $a_1, a_2, \dots, a_{K'}$ not all 0, $\underline{\boldsymbol{a}}^T = [a_1, a_2, \dots, a_{K'}]$ and $\underline{\boldsymbol{0}}^T = [\underbrace{0, 0, \dots, 0}_{K' \text{ elements}}]$. We use (B.4) to prove that there exists a relationship between the elements of vector $\underline{\hat{\boldsymbol{P}}}_\ell$

$$\underline{\boldsymbol{a}}^T\,\underline{\hat{\boldsymbol{P}}}_\ell = \underline{\boldsymbol{a}}^T\,\underline{\hat{\boldsymbol{\Sigma}}}\,\underline{\hat{\boldsymbol{\theta}}} = \underline{\boldsymbol{0}}^T\,\underline{\hat{\boldsymbol{\theta}}} = 0\ . \tag{B.5}$$

It follows that for the K' lines in $\mathscr{K}$, we may at most specify the flows on $K'-1$ lines. As a result, for K lines in $\mathscr{K} \supset \mathscr{K}'$, we may at most specify the flows on $K-1$ lines, which contradicts the proposition statement. □

The result in Proposition 2 implies that $K \leq N$, since the smallest number of lines in a connected network without a loop is always that of a tree.

APPENDIX C

NETWORK TOPOLOGY OF *IEEE* 118-BUS SYSTEM

Figure C.1 shows the network topology of the *IEEE* 118-bus system.

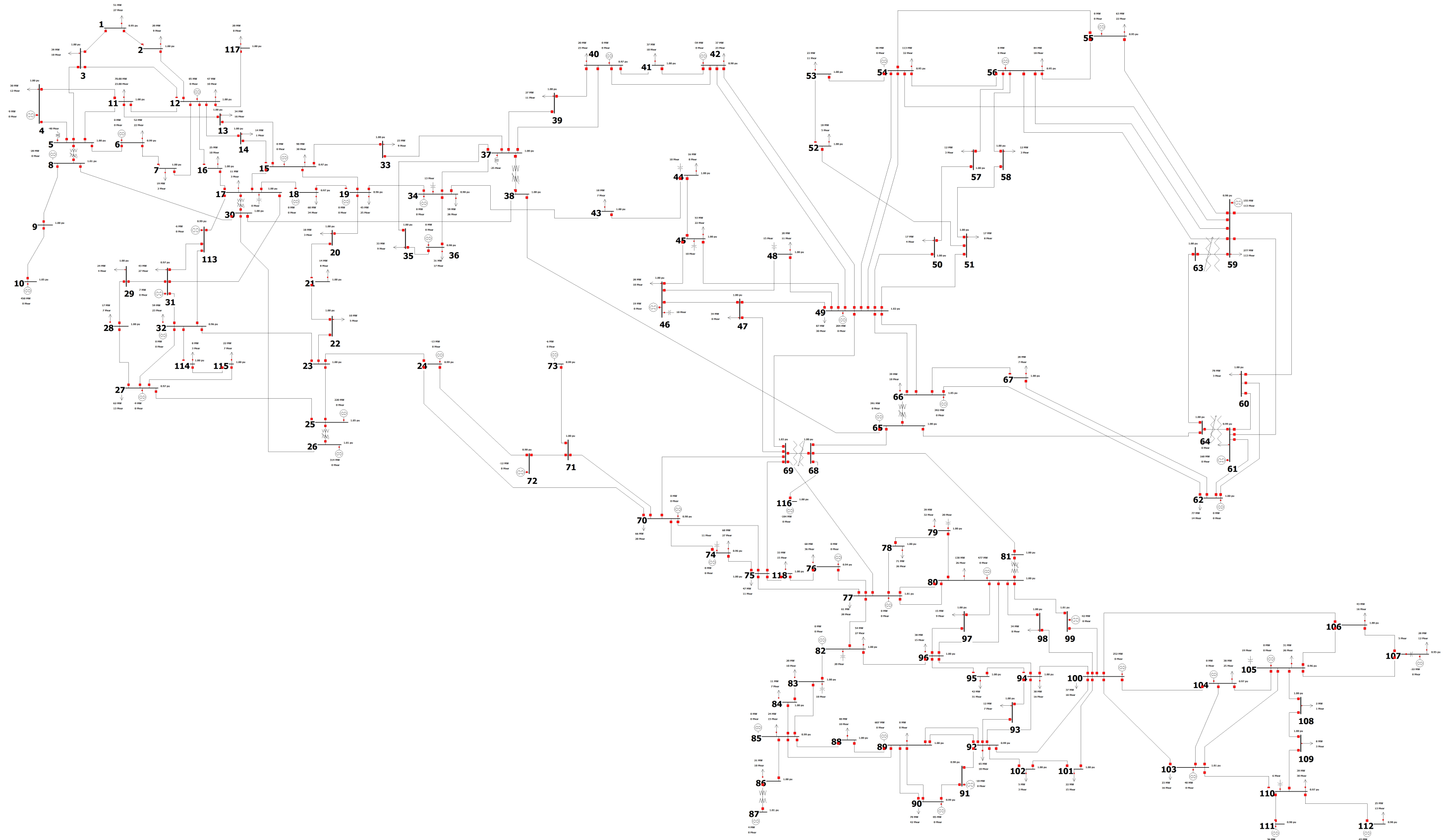

Figure C.1: One line diagram of the *IEEE* 118-bus system

APPENDIX D

DATA USED IN THE APPLICATION STUDIES

Tables D.1-D.2 give the data used in the cases for system R, Tables D.3-D.4 those used in the cases for system R and Table D.5 gives the names of the buses in system T.

Table D.1: Real power flow limits of the 30-bus system

line	maximum real power flow (MW)
$(1,2)$	30
$(6,7)$	5
$(22,24)$	15
$(6,8)$	25
$(12,15)$	20
$(21,22)$	30
remaining lines	100

Table D.2: Lines outages in the period of one month for the 30-bus system

day	line outaged
5	$(27,29)$
6	$(2,6)$
13	$(27,30)$
15	$(10,17)$
24	$(6,10)$
28	$(18,19)$
29	$(29,30)$

Table D.3: Lines outages in the period of one month for the 118-bus system

day	line outaged
15	(1, 3)
17	(80, 98)
19	(105, 106)
20	(18, 19)
21	(105, 107)
23	(76, 77)
24	(14, 15)
25	(37, 40)
26	(110, 111)
27	(100, 104)

Table D.4: Offer curves of generators for half of January in the 118-bus system: $c_i(P_i) = \alpha_1 P_i^2 + \alpha_2 P_i$

node	α_1	α_2
1	0.917	40
4	0.286	40
6	0.757	40
8	0.754	40
10	0.380	20
12	0.568	20
15	0.076	40
18	0.054	40
19	0.531	40
24	0.779	40
25	0.934	20
26	0.130	20
27	0.569	40
31	0.469	20
32	0.012	40
34	0.337	40
36	0.162	40
40	0.794	40
42	0.311	40
46	0.529	20
49	0.166	20
54	0.602	20
55	0.263	40
56	0.654	40
59	0.689	20
61	0.748	20
62	0.451	40

node	α_1	α_2
65	0.084	20
66	0.229	20
69	0.913	20
70	0.152	40
72	0.826	40
73	0.538	40
74	0.996	40
76	0.078	40
77	0.443	40
80	0.107	20
85	0.962	40
87	0.005	20
89	0.775	20
90	0.817	40
91	0.869	40
92	0.084	40
99	0.400	40
100	0.260	20
103	0.800	20
104	0.431	40
105	0.911	40
107	0.182	40
110	0.264	40
111	0.146	20
112	0.136	40
113	0.869	40
116	0.580	40

Table D.5: Names of nodes in $\mathscr{F}_0$ for the *PJM ISO* network

node number	**name**
2276	MASSEY
2416	ALBRIGHT
2512	DRYRUN
2664	MARLOWE
2682	MIRACLER
2710	NLONGVW
2727	OPEQUON
2761	RIDGELEY
2806	SOAKFORD

REFERENCES

[1] T. Orfanogianni and G. Gross, "A general formulation for LMP evaluation," in *IEEE Transactions on Power Systems*, vol. 22, no. 3, August 2007, pp. 1163–1173.

[2] "PJM day ahead energy market outcomes," Accessed Nov. 2011. [Online]. Available: http://www.pjm.com/markets-and-operations/energy/day-ahead.aspx

[3] W. W. Hogan, "Contract networks for electric power transmission," *Journal of Regulatory Economics*, vol. 4, no. 3, pp. 211–42, September 1992. [Online]. Available: http://ideas.repec.org/a/kap/regeco/v4y1992i3p211-42.html

[4] W. W. Hogan, "Financial transmission rights formulations," March 2002. [Online]. Available: www.lecg.com/Portals/0/LECG/Upload/FTRFormulations033102.pdf

[5] "Workshop on *PJM ARR* and *FTR* market 2009/2010," Accessed Nov. 2011. [Online]. Available: http://www.pjm.com/markets-and.../~/.../ftr/2009-annual-ftr-auction-training.ashx

[6] *NYISO* website, Accessed Nov. 2011. [Online]. Available: http://www.nyiso.com/public/markets_operations/services/market_training/library/index.jsp

[7] *MISO* website, Accessed Nov. 2011. [Online]. Available: https://www.midwestiso.org/MARKETSOPERATIONS/MARKETINFORMATION/Pages/FTRMarket.aspx

[8] J. Lally, "Financial transmission rights, auction revenue rights, and qualified upgrade awards," 2010. [Online]. Available: www.iso-ne.com/support/training/courses/wem201/ftr_arr_qua.pdf

[9] T. Kristiansen, "Markets for financial transmission rights," Accessed Nov. 2011. [Online]. Available: www.hks.harvard.edu/.../Kristiansen.mkts.for.ftrs.Oct.03.updated.May.04.pdf

[10] O. Alsac, J. Bright, S. Brignone, M. Prais, C. Silva, B. Stott, and N. Vempati, "The rights to fight price volatility," *IEEE Power and Energy Magazine*, vol. 3, no. 6, pp. 47–57, Jul.-Aug. 2004.

[11] A. Bykhovsky, D. A. James, and C. A. Hanson, "Introduction of option financial transmission rights into the New England market," in *IEEE Power Engineering Society General Meeting*, vol. 1, June 2005, pp. 237 – 242.

[12] T. Li and M. Shahidehpour, "Risk-constrained FTR bidding strategy in transmission markets," *IEEE Transactions on Power Systems*, vol. 20, no. 2, pp. 1014 – 1021, May 2005.

[13] X. Ma, D. Sun, and A. Ott, "Implementation of the PJM financial transmission rights auction market system," in *IEEE Power Engineering Society Summer Meeting*, vol. 3, July 2002, pp. 1360 –1365.

[14] V. Sarkar and S. A. Khaparde, "A robust mathematical framework for managing simultaneous feasibility condition in financial transmission rights auction," in *IEEE Power Engineering Society General Meeting*, 2006, p. 6.

[15] Z. Fan, T. Horger, J. Bastian, and A. Ott, "An overview of PJM energy market design and development," in *Third International Conference on Electric Utility Deregulation and Restructuring and Power Technologies*, April 2008, pp. 12 –17.

[16] P. Ermida, J. Ferreira, Z. Vale, and T. Sousa, "Auction of financial transmission rights in electricity market environment," in *International Conference on the European Energy Market (EEM)*, June 2010, pp. 1 –6.

[17] V. Sarkar and S. A. Khaparde, "A comprehensive assessment of the evolution of financial transmission rights," *IEEE Transactions on Power Systems*, vol. 23, no. 4, pp. 1783–1795, November 2008.

[18] W. W. Hogan, "Restructuring the electricity market: Institutions for network systems," Accessed Nov. 2011. [Online]. Available: http://www.hks.harvard.edu/fs/whogan/hjp0499.pdf

[19] T. Kristiansen, "Merchant transmission expansion based on financial transmission rights," in *Proceedings of the 38th Annual Hawaii International Conference on System Sciences*, January 2005, p. 60b.

[20] M. Patnik and M. Ilic, "Capacity expansion and investment as a function of electricity market structure: Part II - transmission," in *IEEE Power Tech Russia*, June 2005, pp. 1 –7.

[21] S. Oren, G. Gross, and F. Alvarado, "Alternative business models for transmission investment and operation," Accessed Nov. 2011. [Online]. Available: http://www.certs.lbl.gov/ntgs/issue-3.pdf

[22] T. Guler, G. Gross, and M. Liu, "Generalized line outage distribution factors," *IEEE Transactions on Power Systems*, vol. 22, no. 2, pp. 879 –881, May 2007.

[23] M. Liu and G. Gross, "Framework for the design and analysis of congestion revenue rights," *IEEE Transactions on Power Systems*, vol. 19, no. 1, pp. 243 – 251, February 2004.

[24] M. Liu and G. Gross, "Role of distribution factors in congestion revenue rights applications," *IEEE Transactions on Power Systems*, vol. 19, no. 2, pp. 802 – 810, May 2004.

[25] R. Gribonval, R. F. i Ventura, and P. Vandergheynst, "A simple test to check the optimality of a sparse signal approximation," in *Signal Processing*, vol. 86, no. 3, March 2006, pp. 496–510.

[26] D. Donoho and V. Stodden, "Breakdown point of model selection when the number of variables exceeds the number of observations," August 2007. [Online]. Available: www.stanford.edu/~vcs/papers/IJCNN06-1700-dldvcs.pdf

[27] P. Breen, "Algorithms for sparse approximation," 2009. [Online]. Available: www.maths.ed.ac.uk/~s0789798/sparse.pdf

[28] "Power systems test case archive," Accessed Nov. 2011. [Online]. Available: http://www.ee.washington.edu/research/pstca/

[29] "The IEEE reliability test system-1996, a report prepared by the reliability test system task force of the application of probability methods subcommittee," in *IEEE Transactions on Power Systems*, vol. 14, no. 3, 1999.

[30] "Matpower: A Matlab power system simulation package," Accessed Nov. 2011. [Online]. Available: http://www.pserc.cornell.edu/matpower/

[31] J. A. McHugh, *Algorithmic Graph Theory*. Euglewood Cliffs, NJ: Prentice-Hall International Editions, 1990.